Diploma thesis:

Process Design and Optimisation for Continuous Pharmaceutical Manufacturing of Atropine and Diazepam

Author:

Nikolaos Mytis

Supervisors:

Dimitrios Gerogiorgis (UoE, Edinburgh)

Andreas Boudouvis (NTUA, Athens)

NATIONAL TECHNICAL UNIVERSITY OF ATHENS

School of Chemical Engineering

Department of Process Analysis and Design

June 2018

Acknowledgments

I would like to thank my supervisor from the University of Edinburgh, Dr. Dimitrios Gerogiorgis, for his trust and dedication, for helping me stay focused and take initiatives, and for supporting me during my stay in Edinburgh.

I would also like to thank my supervisor from the National Technical University of Athens, Professor Andreas Boudouvis, who introduced me to the opportunity of this Erasmus+ project, and has always been there for me with help and advice.

I am greatly indebted to Mr. Samir Diab, for his tremendous guidance and his continuous feedback throughout this project. This work would never be possible without him and the time he devoted for me.

Special thanks to Dr. Maria-Chiara Ferrari, who handled the procedural matters of my mobility, and to Dr. Gregory Francois, my personal tutor, for his interest for my well-being.

Of course, I am deeply grateful for my parents, who supported me while abroad and have always encouraged me to aim high and expand my academic horizons.

Finally, I would like to express my appreciation to the Erasmus+ program of the European Union, which made this semester at the University of Edinburgh possible by providing me with the grant.

Εκτενής Περίληψη

Η Συνεχής Παραγωγή Φαρμάκων (Continuous Pharmaceutical Manufacturing, CPM) είναι μία νέα μέθοδος παραγωγής ενεργών φαρμακευτικών συστατικών (active pharmaceutical ingredients), η οποία προσφέρει σημαντικά πλεονεκτήματα έναντι των αντίστοιχων ασυνεχών (batch) διεργασιών. Τα πλεονεκτήματα αυτά αφορούν στην απόδοση, την εξοικονόμηση κόστους, τον έλεγχο της διεργασίας και την ασφάλεια. Ο εκσυγχρονισμός της φαρμακευτικής βιομηχανίας μέσω συνεχούς παραγωγής απαιτεί λεπτομερείες τεχνοοικονομικές μελέτες, οι οποίες να καταδεικνύουν εμφανώς τα πλεονεκτήματα της μετάβασης αυτής.

Η σύνθεση σε συνεχή ροή της ατροπίνης και της διαζεπάμης, δύο φαρμακευτικών ουσιών με υψηλές εμπορικές πωλήσεις, έχει ήδη μελετηθεί. Σκοπός της εργασίας αυτής είναι να ερευνηθεί η τεχνική, οικονομική και περιβαλλοντική βιωσιμότητα της συνεχούς διεργασίας παραγωγής των δύο φαρμάκων σε ευρεία κλίμακα. Προς την επίτευξη αυτού του στόχου, οι διεργασίες μοντελοποιούνται σε μόνιμη κατάσταση, αριστοποιούνται και τα αποτελέσματα αναλύονται.

Το διάγραμμα ροής της ατροπίνης έχει βασιστεί στην δημοσίευση της Anne-Catherine Bédard[19]. Η σύνθεση γίνεται σε δύο στάδια. Στο πρώτο στάδιο, λαμβάνει χώρα η εστεροποίηση μεταξύ της τροπίνης και του φαινυλακετυλικού χλωριδίου, προς τον σχηματισμό της τριτοταγούς αμίνης του τροπινικού εστέρα. Η μετατροπή αυτού του σταδίου είναι σχεδόν πλήρης. Στο δεύτερο στάδιο, προστίθεται υδατικό διάλυμα NaOH για την αποπροτονίωση της αμίνης, και υδατικό διάλυμα φορμαλδεΰδης για την σύνθεση της ατροπίνης μέσω αλδολικής προσθήκης. Ο διαχωρισμός του API από τα παραπροϊόντα γίνεται σε ένα στάδιο, με προσαρμογή του pH, ώστε η ατροπίνη να απομονωθεί στο υδατικό ρεύμα.

Το διάγραμμα ροής της διαζεπάμης έχει βασιστεί στην δημοσίευση του H. Samuel Ewan[20] για την σύνθεση της ουσίας σε συνεχή ροή, και γίνεται επίσης σε δύο στάδια. Στο πρώτο στάδιο, παράγεται μια ενδιάμεση αμίνη από αντίδραση ακυλίωσης μεταξύ της 5-χλωρο-2-(μεθυλαμινο)-βενζοφαινόνης και του 2-βρωμοακετυλικού χλωριδίου. Στο δεύτερο στάδιο, προστίθεται αμμωνία για την σύνθεση της διαζεπάμης. Πριν την προσθήκη αμμωνίας, προτείνεται αραίωση του ρεύματος 1:4 με διαλύτη, λόγω της χαμηλής διαλυτότητας της διαζεπάμης. Η μέγιστη απόδοση επιτυγχάνεται με χρήση τολουενίου ως διαλύτη-φορέα. Ο διαχωρισμός γίνεται επίσης σε δύο στάδια. Αρχικά, απομακρύνονται ακαθαρσίες διαλυτές στο νερό, με προσθήκη πολικού διαλύτη (νερού ή προπυλαινικής γλυκόλης). Η διαζεπάμη είναι πρακτικά αδιάλυτη στο νερό και παραμένει στο οργανικό ρεύμα. Έπειτα, απομακρύνονται οι οργανικές ακαθαρσίες, με προσθήκη υδατικού διαλύματος HCl και απομόνωση του API στο υδατικό ρεύμα.

Για την μοντελοποίηση των διαγραμμάτων ροής, αναπτύσσονται κινητικές εκφράσεις και προσαρμόζονται σε δεδομένα μέσω παλινδρόμησης, σχεδιάζονται και διαστασιολογούνται οι αντιδραστήρες εμβολικής ροής (Plug Flow Reactor, PFR), προσομοιώνονται οι διαχωρισμοί φάσεων μέσω του μοντέλου UNIFAC, υπολογίζεται η κατανομή του API στην κάθε φάση με χρήση εμπειρικών σχέσεων ή UNIFAC, υπολογίζεται η απόδοση της εκχύλισης, σχεδιάζονται και διαστασιολογούνται οι μονάδες εκχύλισης υγρού-υγρού και κοστολογείται το εργοστάσιο. Το κόστος περιλαμβάνει λειτουργική δαπάνη (Operational Expenditure, OpEx), ανηγμένη στην παρούσα αξία, και κεφαλαιουχική

δαπάνη (Capital Expenditure, CapEx). Ως μέτρο της περιβαλλοντικής απόδοσης του κάθε εργοστασίου χρησιμοποιείται ο παράγοντας E (E-factor), δηλαδή ο λόγος της μάζας των αποβλήτων προς την μάζα του καθαρού προϊόντος.

Για την αριστοποίηση του μοντέλου, οι μεταβλητές σχεδιασμού (όγκοι αντιδραστήρων, όγκοι διαχωριστήρων, λόγος διαλύτη προς τροφοδοσία, pH εκχύλισης) υπολογίζονται απαιτώντας την ελαχιστοποίηση του συνολικού κόστους για δυναμικότητα εργοστασίου 100 kg API ανά έτος, με χρόνο ζωής 20 έτη. Εξετάζονται διάφορα σενάρια διαλυτών, θερμοκρασιών και ποσοστών ανάκτησης διαλύτη. Υπάρχει μια ισορροπία στο κόστος μεταξύ μετατροπής και μεγέθους αντιδραστήρα, καθώς μεγάλοι χρόνοι παραμονής οδηγούν σε υψηλό CapEx, εξαιτίας αυξημένου όγκου εξοπλισμού, και μικροί χρόνοι παραμονής οδηγούν σε υψηλό OpEx, εξαιτίας αυξημένων αναγκών σε πρώτες ύλες. Η λύση είναι ευαίσθητη στις τιμές των πρώτων υλών, ειδικά των διαλυτών. Το συνολικό κόστος επηρεάζεται έντονα από την ανάκτηση του API κατά τα στάδια του διαχωρισμού. Η μέγιστη δυνατή ανάκτηση του API είναι συνήθως επιθυμητή, καθώς το κόστος του διαχωριστήρα δεν είναι σημαντικό και δεν υπάρχει αντίστοιχη ισορροπία όπως με τους αντιδραστήρες.

Η συνεχής παραγωγή της ατροπίνης είναι αρκετά αποδοτική, εξαιτίας των εξαιρετικά συγκεντρωμένων ή και καθαρών ρευμάτων που χρησιμοποιούνται. Η επιλεκτικότητα του διαχωρισμού επιτρέπει την επίτευξη υψηλής καθαρότητας, ελαχιστοποιώντας την ανάγκη για επιπλέον καθαρισμό. Η συνεχής παραγωγή διαζεπάμης υπό τις συγκεκριμένες συνθήκες αντίδρασης που μελετήθηκαν δεν είναι αποδοτική, καθώς η χαμηλή της διαλυτότητα απαιτεί μεγάλες ποσότητες διαλυτών-φορέων και, ακολούθως, διαλυτών εκχύλισης. Αυτό μεταφράζεται σε υψηλά λειτουργικά κόστη και υψηλό παράγοντα E. Υπάρχουν ωστόσο εναλλακτικές μέθοδοι συνεχούς σύνθεσης της διαζεπάμης οι οποίες είναι υποσχόμενες.

Αποτελέσματα για συνεχή παραγωγή ατροπίνης

Μελετώνται οι περιπτώσεις 50% και 70% ανάκτησης διαλυτών, 90% και 95% καθαρότητας προϊόντος, και η χρήση τολουενίου, διαιθυλαιθέρα και κ-οξικού βουτυλίου ως διαλυτών εκχύλισης. Το κόστος μειώνεται για αύξηση της ανάκτησης διαλύτη. Η καθαρότητα εισάγεται στο πρόβλημα ως περιορισμός, και η απαίτηση για 90% καθαρότητα οδηγεί χαμηλότερο κόστος και παράγοντα E, λόγω μεγαλύτερης ανάκτησης API. Ο διαλύτης με το χαμηλότερο κόστος σε κάθε περίπτωση καθαρότητας είναι το τολουένιο (6.40×10^5 GBP και 6.76×10^5), καθώς η χρήση του επιτυγχάνει την μεγαλύτερη ανάκτηση και έχει την πιο χαμηλή τιμή αγοράς. Για καθαρότητα 90%, ο διαιθυλαιθέρας εμφανίζει χαμηλότερο κόστος από το κ-οξικό βουτύλιο, ενώ για 95% καθαρότητα, η σχέση αυτή αντιστρέφεται. Ο διαλύτης με τον χαμηλότερο παράγοντα E για 90% καθαρότητα είναι ο διαιθυλαιθέρας (6.8), ενώ για 95% καθαρότητα είναι το τολουένιο (8.7). Λαμβάνοντας υπόψη την τοξικότητα των διαλυτών, η χρήση του κ-οξικού βουτυλίου είναι η πιο ακίνδυνη, ενώ η χρήση του διαιθυλαιθέρα συνήθως αποφεύγεται λόγω χαμηλού σημείου ανάφλεξης.

Για 70% ανάκτηση διαλύτη, ο βέλτιστος χρόνος παραμονής στον 2^o αντιδραστήρα κυμαίνεται από 16 έως 19 λεπτά. Όταν υπάρχει απαίτηση για υψηλή καθαρότητα, ο χρόνος παραμονής αυξάνεται, για να μειωθεί η μάζα των ουσιών που δεν αντέδρασαν. Ο βέλτιστος λόγος διαλύτη προς τροφοδοσία κυμαίνεται από 0.4 έως 0.8. Το βέλτιστο pH περιορίζεται σε βασικές τιμές λόγω της απαίτησης για

συγκεκριμένη καθαρότητα, και αυξάνει με την καθαρότητα. Για την περίπτωση με το ελάχιστο κόστος, το βέλτιστο pH είναι 7, που σημαίνει ότι ο διαχωρισμός μπορεί να λάβει χώρα σε ουδέτερες συνθήκες και πιθανώς να μην απαιτεί ρύθμιση του pH. Για 50% ανάκτηση διαλύτη, οι συνθήκες του διαχωρισμού δεν αλλάζουν σημαντικά. Ωστόσο, ο χρόνος παραμονής στον αντιδραστήρα είναι υψηλός και περιορίζεται από το άνω όριο των 24 λεπτών. Αυτό συμβαίνει για να αυξηθεί η απόδοση και να μειωθεί η μαζική ροή της διεργασίας. Το OpEx συμβάλλει περισσότερο στο συνολικό κόστος στην περίπτωση της 50% ανάκτησης.

Αποτελέσματα για συνεχή παραγωγή διαζεπάμης

Μελετώνται οι περιπτώσεις 50% και 70% ανάκτησης διαλυτών, θερμοκρασίες εκχύλισης 25 ^{o}C και 40 ^{o}C, και η χρήση διαλύματος HCl συγκέντρωσης 3M, 4M και 5M για τον δεύτερο διαχωρισμό. Το συνολικό κόστος αυξάνει με την μείωση της συγκέντρωσης του διαλύματος HCl, λόγω της μειούμενης ανάκτησης API στο υδατικό ρεύμα. Η επίδραση της θερμοκρασίας στην ανάκτηση δεν είναι σημαντική, οπότε ο διαχωρισμός είναι προτιμότερο να γίνει στους 40 ^{o}C, ελαχιστοποιώντας τις ανάγκες για ψύξη. Το ελάχιστο κόστος επιτυγχάνεται με χρήση HCl 5M στους 25 ^{o}C και είναι 33.7x10^{5} GBP. Εξαιτίας των υψηλών απαιτήσεων της διεργασίας σε διαλύτες, η μείωση της ανάκτησης διαλύτη από 70% σε 50% επιφέρει σημαντική αύξηση στο κόστος. Οι παράγοντες E ακολοθούν την ίδια τάση με το κόστος και είναι εξαιρετικά υψηλοί, ακόμα και για φαρμακευτικές διεργασίες, με τον ελάχιστο να είναι 146.

Για όλες τις περιπτώσεις, οι χρόνοι παραμονής στους αντιδραστήρες οδηγούνται στα άνω όρια (1 λεπτό, 0.64 λεπτά) και ο βέλιστος λόγος διαλύτη προς τροφοδοσία κυμαίνεται μεταξύ 0.25 και 0.4. Ο λόγος αυτός αυξάνει με μείωση της συγκέντρωσης HCl, για να αντισταθμιστεί η πτώση στην ανάκτηση API. Επίσης, ο λόγος αυξάνει στην περίπτωση της 50% ανάκτησης διαλύτη, κάτι το οποίο οδηγεί σε αύξηση της μαζικής ροής του διαλύτη εκχύλισης μεν, αλλά παράλληλα αυξάνει την ανάκτηση API και οδηγεί σε μείωση της μαζικής ροής του διαλύτη-φορέα. Έτσι, ενώ το OpEx αυξάνεται σημαντικά για μείωση της ανάκτησης διαλύτη από 70% σε 50%, το CapEx μικραίνει, λόγω μείωσης της συνολικής μαζικής ροής της διεργασίας.

Abstract

Continuous Pharmaceutical Manufacturing (CPM) is a modern industrial paradigm for the production of active pharmaceutical ingredients, providing significant benefits over its batch counterpart, including increased efficiency, cost savings, quality control and safety. The transformation of the pharmaceutical industry requires detailed technoeconomic evaluations. The continuous flow synthesis of atropine and diazepam, two popular drugs with high global sales, has been recently demonstrated. In this work, a CPM flowsheet model is established and optimised for each API, featuring novel kinetic expressions fitted to data, reactor design, separation thermodynamics, mass transfer, liquid-liquid extraction design and costing. Several design variables are calculated by minimising the total cost for a plant with capacity of 100 kg API per annum and a lifetime of 20 years. Different solvents, temperatures and solvent recovery percentage cases are considered. The results are then analysed in order to demonstrate the feasibility of the plants. It was found that the continuous production of atropine is efficient, achieving low operational cost, wastage and E-factors, and yielding high purity. The continuous production of diazepam is not efficient, based on continuous flow chemistry used in this work, as it results in excessive solvent use. There are however promising alternative methods for its continuous production.

Contents

Table of Figures

1 Introduction

Until recently, the majority of the pharmaceutical industry relied on batch manufacturing. While batch processes have advantages such as less expensive construction and start-up costs, equipment flexibility and the ability for batch recall, they suffer from large equipment capacities, reduced heat and mass transfer efficiency, poor scaling, quality errors and high waste generation. It is estimated that the pharmaceutical industry wastes $50 billion a year due to inefficient manufacturing[1]. This, along with the recent shortage in drug supply in the US[2] and the increasing R&D costs[3] are driving companies to adopt more efficient production methods.

Continuous pharmaceutical manufacturing, a new production paradigm, could be the solution to the current inefficiencies of the pharmaceutical industry; it allows for a significant reduction in capital and operating costs, manufacturing footprint, waste and downtime, while also increasing the speed to the market. Pharmaceutical firms who implement a continuous manufacturing method could save between 40 and 50 percent in CapEx and OpEx. Of course, cost alone would not matter if continuous manufacturing compromised quality: the high degree of control required for maintaining product quality can only be realised in a steady state, by applying QbD principles.

Recent advances in continuous flow chemistry have enabled the continuous synthesis of a variety of active pharmaceutical compounds (APIs) in various scales[4-6]. One of the benefits of using micro-reactors is the access over new processing windows, allowing for the operation at high pressure and temperature[7], while minimising safety hazards[8]. In addition, there has been investigation of new synthetic routes in continuous flow, involving solvent-free conditions using neat or molten reagents[9]. Around 30-50% of the current batch processes can be converted to continuous while offering benefits over the batch mode. Some manufacturers have already invested in this new technology. In 2015, Janssen became the first company to be approved by the FDA to switch from batch to continuous manufacturing for the HIV drug Prezista[14]. However, due to the current business model of pharma and the prevailing regulatory environment, this shift is slow and requires research conclusively highlighting the benefits of CPM.

Process modeling and simulation are fast and low-cost methodologies for evaluating the feasibility and viability of CPM processes, while also allowing for optimisation. As the projected savings largely depend on reactor and separation design, it is essential to model reaction kinetics from continuous-flow chemistry data and analyse mixture thermodynamics for API purification. A previous study has explored and optimised the performance of continuous synthesis and separation design for ibuprofen by minimizing the total cost of the CPM processes over a certain plant lifetime[15]. Dynamic models have also been developed that allow for plant-wide optimisation[16,17]. Until now, there have been few demonstrations of end to end CPM processes[10,11]. Further research needs to be done on continuous purification and downstream processing of chemical compounds, as the current solutions and modelling tools are limited[12,13].

An important API the production of which can be converted from batch to continuous is atropine. The drug belongs to the class of compounds known as alkaloids and is commonly administered as atropine or its salt, atropine sulphate. It is used for saliva, sweat and mucus secretion, pupil dilation, to treat bradycardia and as an antidote for poisoning with organophosphate nerve toxins, like sarin. Atropine

occurs naturally in the plant Atropa belladonna, from which it was first extracted in crystal form in 1831. It was first synthesised by Richard Willstätterm (Nobel, 1915) and the most common synthetic route involves the reaction of tropine with tropic acid, in the presence of hydrochloric acid. However, currently known processes for synthetically producing atropine or atropine sulfate suffer from a number of disadvantages that make the synthesis impractical on a commercial scale. This is primarily due to the inefficiency of the reactions involved. For that reason, natural product extraction is still preferred over chemical synthesis as an industrial method of atropine production.

Another promising API candidate is diazepam, a drug that is used for the short-term relief of anxiety disorders and symptoms of alcohol withdrawal. It belongs to the benzodiazepine family, a group of central nervous system depressants. First marketed as Valium in 1968, it has been one of the most prescribed medications worldwide. After the patent's expiration in 1985, over 500 different brands of generic diazepam are now sold. Despite several regulatory restrictions imposed in the use of benzodiazepines during the 90s, legitimate prescriptions of diazepam in the US increased by 6% between 2006 and 2012[18]. Benzodiazepines are still considered first line treatment for most other anxiety disorders and phobias.

The aim of this work is to evaluate the technical, economic and environmental performance of the continuous manufacturing of these two APIs: atropine and diazepam. Towards this objective, the steady-state flowsheet model of both processes is developed and optimised, based on the demonstrated continuous flow synthesis in the literature[19,20]. Novel kinetic expressions are formulated, parameters are estimated with regression analysis and plug flow reactor design is conducted. For the purification stages, both experimental and theoretically derived solubilities and distribution factors are used. The liquid-liquid extraction efficiency is then modelled and the recovery of the APIs is calculated. The model is costed taking into consideration CapEx and Opex, while environmental efficiency is evaluated using the E-factor. Finally, the model is optimised under different cases and constraints. The results with the mass balances are presented and discussed for a plant capacity of 100 kg API per year.

2 Process modelling

2.1 Flowsheet development

2.1.1 Atropine

Continuous-flow synthesis of atropine in micro-scale has been demonstrated twice by the same group, first by Chunhui Dai[21] and later by Anne-Catherine Bédard[19], who optimised the process. The reported synthesis of atropine begins with the esterification reaction between tropine and phenylaceyl chloride, to give the tertiary amine of tropine ester. Almost total conversion is achieved in this reaction. Next, aqueous solution of NaOH is added to deprotonate the amine of the ester and give tropine ester. Finally, an aqueous solution of formaldehyde is added for the aldol addition reaction, to give atropine. The authors also explore the separation of atropine from the byproducts, based on their pKa difference, by adjusting the pH of the aqueous solution during the liquid-liquid extraction.

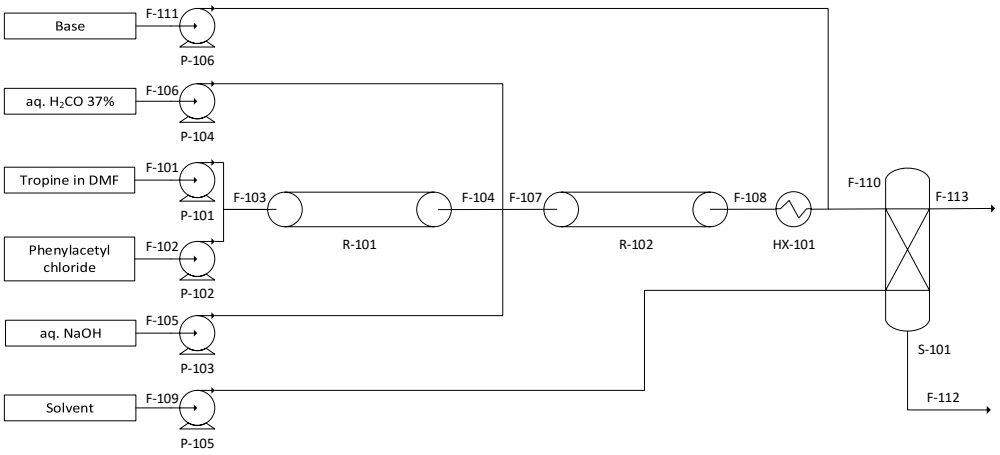

Figure 1. Atropine synthesis and purification process flowsheet.

2.1.2 Diazepam

Continuous-flow synthesis of diazepam has been demonstrated by H. Samuel Ewan et al[20]. It begins with the N-acylation reaction of 5-chloro-2-(methylamino)benzophenone with 2-haloacetyl chloride, giving an intermediate amide. Next, ammonia is added for the cyclization reaction, which gives diazepam. The reactants are dissolved in toluene, NMP or ACN, while ammonia is dissolved in methanol. Due to the low solubility of diazepam after the addition of ammonia/methanol, the authors suggest an extra 1:4 dilution step with the solvent before the second reaction. The highest yield is achieved with the use of bromoacetyl chloride as reactant and toluene as solvent. Two liquid-liquid extractions are then employed, in order to remove inorganic and organic impurities.

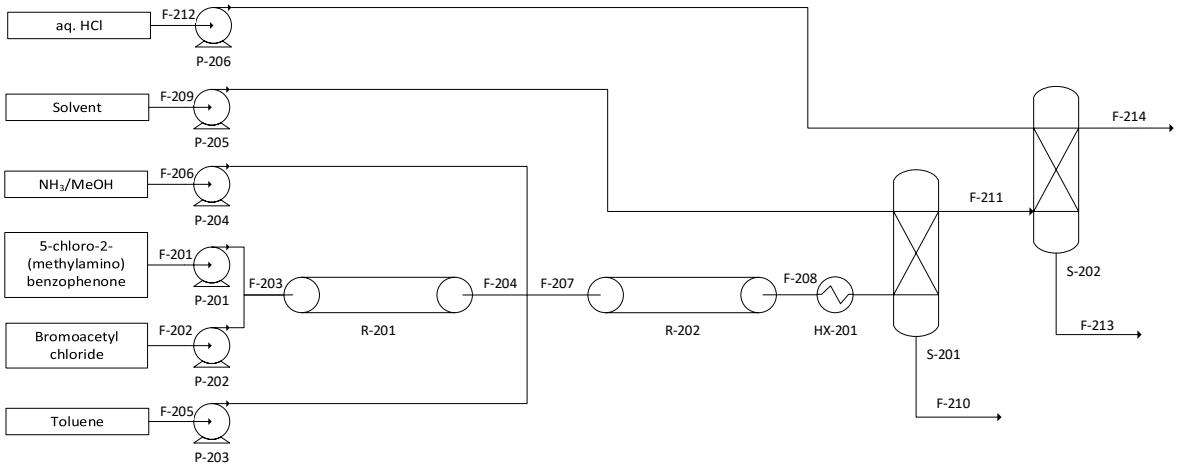

Figure 2. Diazepam synthesis and purification process flowsheet.

2.2 Reaction scheme and kinetics

2.2.1 Atropine

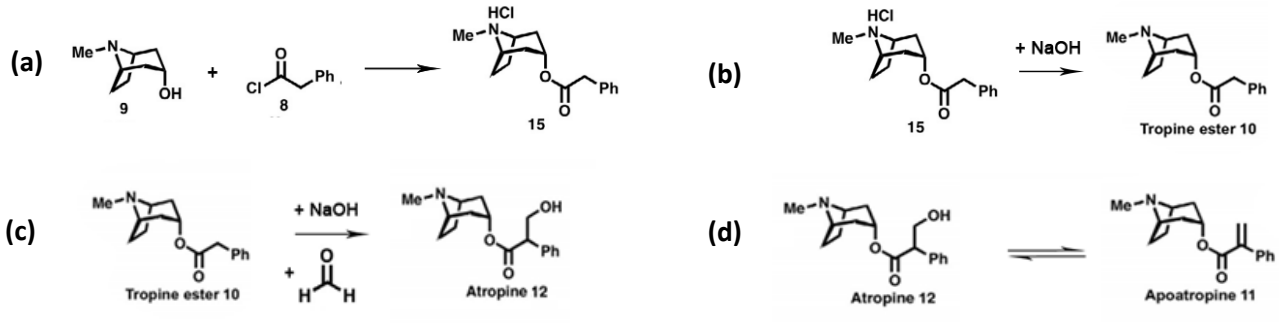

Figure 3. Reaction path for the synthesis of Atropine: (a) Esterification of phenylacetyl chloride **8** with tropine **9** to form the tertiary amine of tropine ester **15**, (b) Deprotonation of the amine of tropine ester **15** to form tropine ester **10**, (c) Aldol (H_2CO) addition on the tropine ester **10** to form atropine **12**, (d) Degradation of atropine **12** to apoatropine **11**.

In the first reactor, the esterification of phenylacetyl chloride 8 with tropine 9 forms the tertiary amine of tropine ester 15. This reaction not modelled in this study, due to lack of experimental data. Its conversion is assumed to be 99% under the same conditions as in the original continuous experiment.

The effluent stream of the first reactor is mixed with NaOH, to deprotonate the amine into tropine ester 10. This reaction is considered to be instant and to full extent, as it is an acid-base reaction. In the second reactor, formaldehyde is added to **10** to form atropine **12**. This reaction is catalyzed by NaOH and two candidate mechanisms are suggested. The first is the simple mechanism, completed in the following steps[22]:

a. $10 + \mathrm{OH}^- \leftrightarrow 10^- + \mathrm{H_2O}$
b. $10^- + \mathrm{H_2CO} \rightarrow 12^-$
c. $12^- + \mathrm{H_2O} \rightarrow 12 + \mathrm{OH}^-$

The steady-state approximation for the intermediates yields:

$$-\mathrm{r}_{10} = \mathrm{k}_{102} C_{10}^{*} C_{H_2CO} \qquad (1)$$

However, when catalytic amounts of base (NaOH) are used, it is reported that the deprotonization of **10** happens when interacting with the anion of **12**[21]. So, the first step becomes:

a'. $10 + 12^- \leftrightarrow 10^- + 12$

And the steady-state approximation for the intermediates yields:

$$-\mathrm{r}_{10} = k_{102}\frac{C_{10}C_{H_2CO}}{C_{10,0}-C_{10}} \qquad (2)$$

Finally, atropine 12 is partially converted to apoartopine 11, under an equilibrium process[23]:

$$\mathrm{K}_{\mathrm{eq}} = \frac{\mathrm{C}_{11}}{\mathrm{C}_{12}} \qquad (3)$$

2.2.2 Diazepam

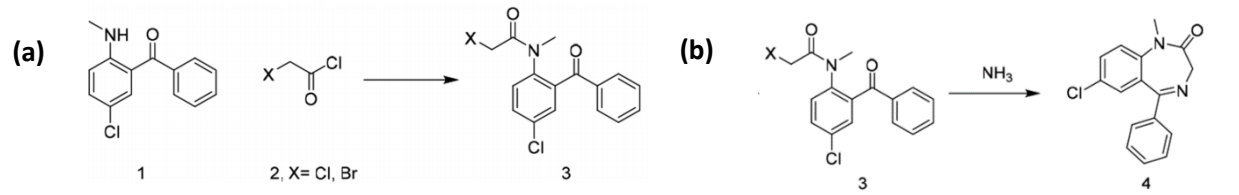

Figure 4. Diazepam synthesis reaction path: (a) N-acylation of 5-chloro-2-(methylamino)benzophenone **1** with 2-haloacetyl chloride **2** giving amide **3**, (b) Cyclization of amide **3** to give Diazepam **4**.

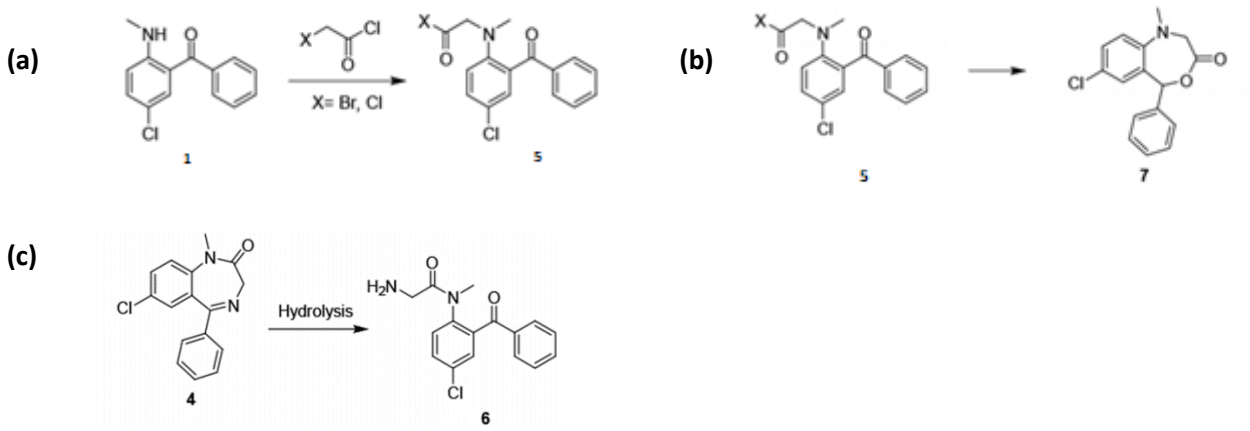

Figure 5. Diazepam synthesis side reactions**:** (a) N-acylation of **1** to **5**, which cannot yield Diazepam **4**, (b) Formation of byproduct **7** from **5**, (c) Hydrolysis of Diazepam **4** to byproduct **6**.

In the first reactor, an amidation reaction between 5-chloro-2-(methylamino)benzophenone **1** and bromoacetyl/chloroacetyl chloride **2** yields intermediate **3**. The three candidate expressions for this reaction are:

$$r_1 = k_{201} C_1 C_2 \quad (4)$$

$$r_1 = k_{201} C_1 \quad (5)$$

$$r_1 = k_{201} \quad (6)$$

for second-order, first-order and zeroth-order kinetics, respectively.

In the second reactor, ammonia is added to cyclise intermediate **3** into diazepam **4**. The three candidate expressions are:

$$r_3 = k_{202} C_3 C_{NH_3} \quad (7)$$

$$r_3 = k_{202} C_3 \quad (8)$$

$$r_3 = k_{202} \quad (9)$$

for second-order, first-order and zeroth-order kinetics, respectively.

2.3 Kinetic parameter estimation and PFR design

The residence time of a plug flow reactor is calculated using the integral form of the molar mass balance:

$$\tau = \mathrm{C}_{i,0} \int_0^{\mathrm{x_i}} \frac{\mathrm{dx}}{-\mathrm{r_i}} \quad (10)$$

where subscript i denotes the reactant species, $c_{i,0}$ is the initial concentration of i, x is the conversion of i and r_i is the rate of disappearance of i.

When the required conversion and the rate law of the reaction are known, the volume of the reactor is calculated as:

$$V = Q \cdot \tau \quad (11)$$

where Q is the volumetric flow through the reactor, estimated as:

$$Q = \sum_i \frac{\dot{m}_\iota}{\rho_\iota} \quad (12)$$

where $\dot{m}_\iota$ is the mass flow of i through the reactor and ρ_i is the density of i. The effects of temperature and mixing on volume are out of the scope of this study and have not been considered.

When continuous-flow experimental data of product composition at different residence times is available, the RHS of eq. (10) is plotted against time, which results in a linear correlation with slope k:

$$k\tau = y(x) \quad (13)$$

Different rate expressions are tested to determine the order of each reaction, using the coefficient of determination (R^2) as a measure of the goodness of the fit.

2.3.1 Atropine

For the continuous-flow synthesis of atropine **12**, data published by Bédard et al is used[19]. The esterification step is conducted at 100 °C, for varying residence times (10, 7.5, 3.5 minutes), using **9** (2M in DMF), varying equivalents of **8** (1.00, 1.05, 1.10) and varying concentrations of **8** (2.0 M in DMF solution, 7.6 M neat). When using a neat **8** stream and a **9** stream near saturation point, 99% conversion is achieved for residence times greater than 3.5 minutes.

The aldol addition step is conducted at 100 °C for varying residence times (8, 24 minutes), using 6 equivalents of H_2CO in 37% w/w aq. solution, varying NaOH concentrations (1, 3 M) and varying NaOH equivalents (1.2, 3). The highest yield is achieved when using 1.2 equivalents of NaOH 3M solution.

For the formation of the amine of tropine ester **15**, the experimental data does not suffice for the derivation of a kinetic expression. The minimum residence time for which 99% conversion is obtained is used for calculations:

$$\tau_{101} = 3.5\ min \qquad (14)$$

For the conversion of tropine ester **10** to atropine **12**, both non-catalytic and catalytic rate expressions are plotted against time. Pseudo-first-order (1st in **10**, 1st in formaldehyde, -1st in **12**) reaction is the most plausible (R^2 = 0.8855), compared to second-order reaction (R^2 = 0.7569). This result confirms the catalytic mechanism hypothesis for the aldol addition reaction, with k_{102} = 0.0061 min^{-1}.

The PFR design equation becomes:

$$\tau_{102} k_{102} = C_{10,0} \int_0^x \frac{dx}{\frac{C_{10,0}(1-x)\left(C_{H_2CO,0} - C_{10,0}x\right)}{C_{10,0}x}} \qquad (15)$$

Eq. (15) cannot be solved analytically for x, so numerical integration is used.

For the degradation of atropine **12** to apoatropine **11**, it is observed that the experimental ratio of $\frac{C_{11}}{C_{12}}$ is almost identical for residence times of 8 and 24 minutes. Thus, it is assumed that the equilibrium process is fast, and the constant is calculated from the ratio of the two compounds:

$$K_{eq} = \frac{C_{11}}{C_{12}} = 0.64 \qquad (16)$$

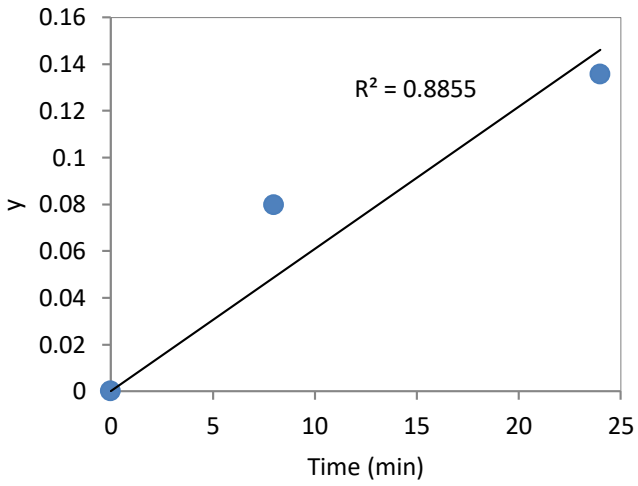

Figure 6. Kinetic parameter estimation from experimental data for reaction $10 + H_2CO \rightarrow 12$ (100 °C)

Table 1. Atropine synthesis reaction summary as a basis for reactor design

	R-101	R-102	R-102	R-102
Reaction	$8 + 9 \rightarrow 15$	$15 + NaOH \rightarrow 10$	$10 + H_2CO \rightarrow 12$	$12 \leftrightarrow 11$
Reaction type	Esterification (full)	Acid-Base (full)	Aldol addition	Equilibrium
Reaction order	-	Instant	pseudo-1st	-
Reactor temperature (°C)	100	100	100	100
Rate/equilibrium constant	-	-	0.0061 min^{-1}	0.64
R^2	-	-	0.886	-

2.3.2 Diazepam

For the continuous-flow synthesis of diazepam, data published by Ewan et al is used[20]. The intermediate synthesis step is conducted at 75 °C, for varying residence times (1, 2 minutes), using different solvents (toluene, ACN). The diazepam synthesis step is conducted at varying temperatures (100, 110, 120, 130, 140, 150 °C), for varying residence times (0.32, 0.64 minutes), using different solvents (Toluene, ACN, NMP). The highest yield is achieved when using bromoacetyl chloride as reactant, at 75 °C for the first reaction and 120 °C for the second reaction, and toluene as the common solvent. For this case, the

composition of the product contains only traces of byproducts **5**, **6**, **7**, so all side-reactions occurring at these conditions can be considered negligible.

The full continuous-flow experiment described does not provide enough data for the synthesis of the intermediate **3**, so data from the microfluidic one-step synthesis of intermediate **3** is used. The one-step experiment is performed for temperatures of 50, 100, 150 °C, residence times of 30, 60, 180 seconds and different solvents (Toluene, ACN). For residence times between 60 and 180 seconds, high concentration of byproduct **6**, regardless of temperature. This suggests that hydrolysis of the product occurs at high residence times. Consequently, data at 180 seconds is not considered for the purpose of regression.

For temperatures higher than 50 °C, there is formation of reactant **1** and consumption of intermediate product **3** after 30 seconds. This observation suggests the existence of side-reactions at high temperature conditions, and thus only data at 50 °C can be used for rate constant estimation for the assumption of negligible side-reactions to be valid.

For the synthesis of intermediate **3**, both second-order (first-order in **1**, first-order in **2**) reaction (R^2 = 0.9838) and first-order in **1** reaction (R^2 = 0.9737) are plausible, compared to zeroth-order reaction (R^2 = 0.8514). The single-step mechanism of acylation and the fact that the concentrations of the reactants are equal for this experiment imply that second-order rate is the most plausible, with k_{201} = 117.87 L mol^{-1} min^{-1}.

The PFR design equation for equal and non-equal initial concentrations becomes respectively:

$$k_{201}\tau_{201} = \frac{1}{C_{1,0}(1-x)} - \frac{1}{C_{1,0}} \quad (17)$$

$$k_{201}\tau_{201} = \frac{1}{C_{2,0}-C_{1,0}} ln\left[\frac{(C_{2,0}-C_{1,0}x_1)C_{1,0}}{C_{1,0}(1-x_1)C_{2,0}}\right] \quad (18)$$

For the kinetics of the synthesis of diazepam from intermediate **3**, complete conversion of **1** to **3** is assumed for the first step. Both second-order (first-order in **3**, first-order in ammonia) reaction (R^2 = 0.9890) and first-order reaction (R^2 = 0.9855) are plausible, compared to zeroth-order reaction (R^2 = 0.9133). Given the small molecular size of ammonia compared to that of **3**, and the 7-fold excess of ammonia, it is reasonable to assume that the rate is not affected by the concentration of ammonia, thus a first-order reaction is implemented, with k_{202} = 2.1194 min^{-1}.

The PFR design equation becomes:

$$k_{202}\tau_{202} = ln(\frac{1}{1-x_2}) \quad (19)$$

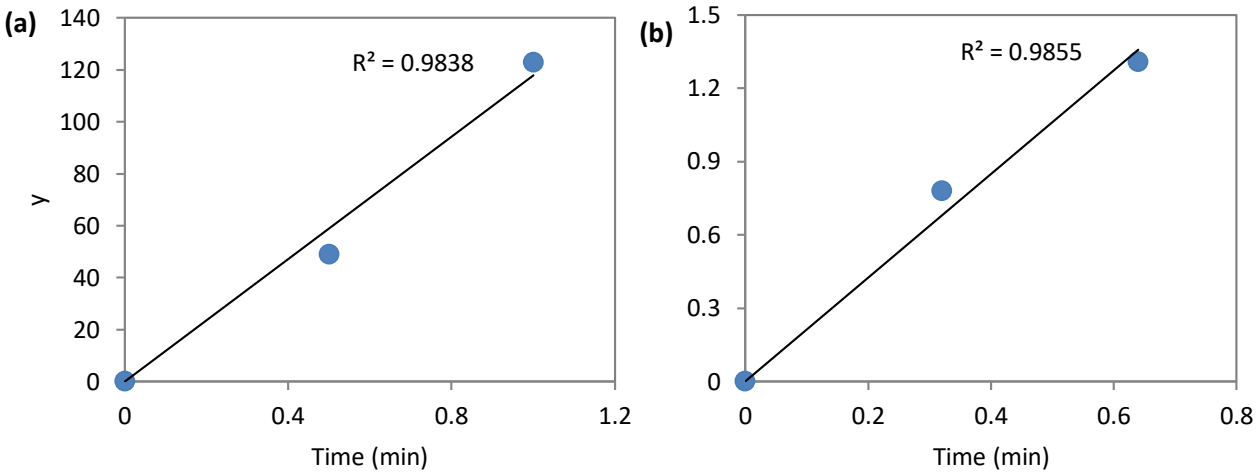

Figure 7. Parameter estimation from experimental data for diazepam synthesis reactions. (a) Reaction $1 + 2 \rightarrow 3$ (50 °C), (b) Reaction $3 + NH_3 \rightarrow 4$ (120 °C).

Table 2. Diazepam synthesis reaction summary as a basis for reactor design

	R-201	R-202
Reaction	$1 + 2 \rightarrow 3$	$3 + NH_3 \rightarrow 4$
Reaction type	N-acylation	Cyclization
Reaction order	2	1
Reactor temperature (°C)	50	120
Rate constant	117.87 (L mol^{-1} min^{-1})	2.119 (min^{-1})

2.4 Separation thermodynamics

The product streams exiting the reactors are binary systems contain the API and a number of other dissolved solutes. In order to purify the product, continuous liquid-liquid extraction (LLE) is implemented. The ternary liquid-liquid equilibria are modelled using UNIFAC. Several candidate extraction solvents are considered for each separation. The addition of the solvent must yield two-phase mixture, and the API must show greater affinity to the solvent than the other solutes.

When the API is insoluble in the extraction solvent, or when the impurities exhibit the same level of solubility as the API, then acid-base extraction is considered. In acid-base extraction, a water-insoluble

molecule is transferred to the aqueous phase, by ionising the compound (adding or removing a proton). It used to separate organic compounds based on their pKa differences[24]. In this study, both APIs behave as weak bases.

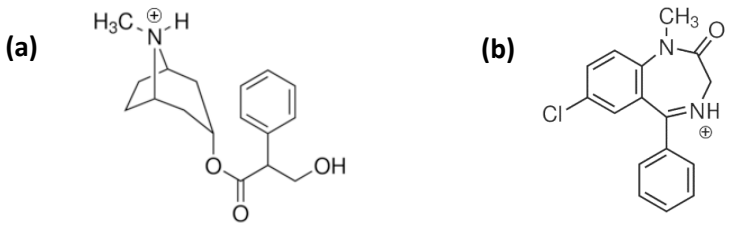

Figure 8. Protonated forms of (a) Atropine, (b) Diazepam.

The partitioning of the compounds between the two phases is calculated using the distribution coefficient:

$$D = \frac{C_{i,org}}{C_{i,aq}} \quad (20)$$

where $C_{i,org}$ is the sum of the concentrations of i in ionized and non-ionized form in the organic phase and $C_{i,aq}$ is the sum of the concentrations of i in ionized and non-ionized form in the aqueous phase.

For atropine and its impurities, the distribution coefficients against the pH of the solution are computed in various solvents, using SPARC computational software, and are given in the original paper[19]. For diazepam and other compounds, the distribution coefficients are estimated be equal to the ratio of their solubility in the organic phase to their solubility in the aqueous phase.

$$D = \frac{S_{i,org}}{S_{i,aq}} \quad (21)$$

Specifically for diazepam, it is assumed that the ionized form is insoluble in the organic phase and that the non-ionized form is insoluble in the aqueous phase[25].

The maximum recovery of each compound in the aqueous stream is then calculated as:

$$R_{max,i,aq} = \frac{1}{1+\frac{Q_{org}}{Q_{aq}}D} \quad (22)$$

Where $\mathrm{Q_{org}}$ is the volumetric flow of the organic stream and $\mathrm{Q_{aq}}$ is the volumetric flow of the aqueous stream.

2.4.1 Atropine

The product stream exiting PFR II is a binary solution of water (45%) and DMF (29%). Apart from atropine, the stream contains several impurities; formaldehyde, byproducts (apoatropine **11**, tropine ester **10**) and traces of unconverted reactants (tropine **9**, phenylacetyl chloride). In order to remove the impurities, liquid-liquid extraction is performed by adding an extraction solvent and adjusting the pH of the product stream. The API is then collected in the aqueous stream, while the impurities remain in the organic stream.

The computational results[19] (Figure 9) show that compounds **10**, **12** reside mostly in the organic stream for pH > 6, while **12**, **9** reside mostly in the aqueous stream for pH < 8. This indicates that the separation of the API from the impurities by adjusting the pH is indeed feasible, under slightly acidic or slightly basic conditions. Under basic conditions, it is also possible to separate **12** from **9**, but the residual amount of **9** from the synthesis process is minimal, so only one liquid-liquid extraction is enough.

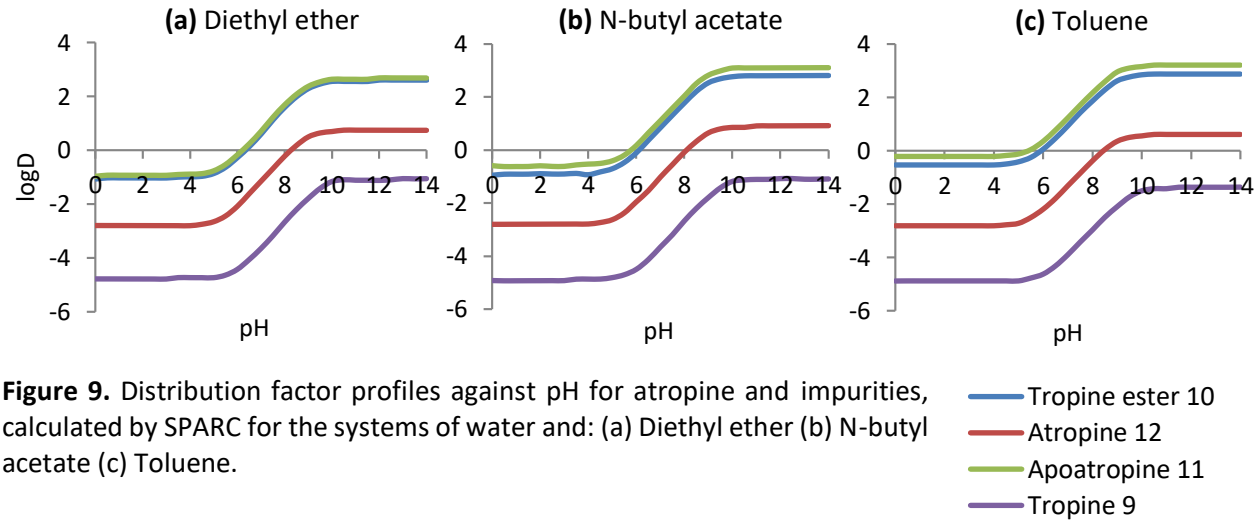

Figure 9. Distribution factor profiles against pH for atropine and impurities, calculated by SPARC for the systems of water and: (a) Diethyl ether (b) N-butyl acetate (c) Toluene.

Surrogate equations for the logarithm of the distribution coefficient for each solvent as a function of the pH are fitted to the data and incorporated into the model. The equations are applicable only for the pH spectrum where the separation is feasible, which corresponds to the linear slope of the $logD$ graph, thus further simplifying the model.

The system water-DMF-solvent is ternary and does not yield pure component phases. In order to use the computed distribution factors for the calculation of the recoveries, the following assumptions were made:

a) The distribution coefficient is not affected by the presence of DMF in the aqueous phase, which is equivalent to the pK_a remaining constant in the aqueous phase. The pK_a in the mixture of water and DMF can be considered fairly constant when the molar fraction of DMF is low and the ionization of the compound (weak base) does not change the total number of ions in the solution $(HB^+ \rightarrow B + H^+)$ [26,27].

b) The distribution coefficient is not affected by the presence of water and DMF in the organic phase.

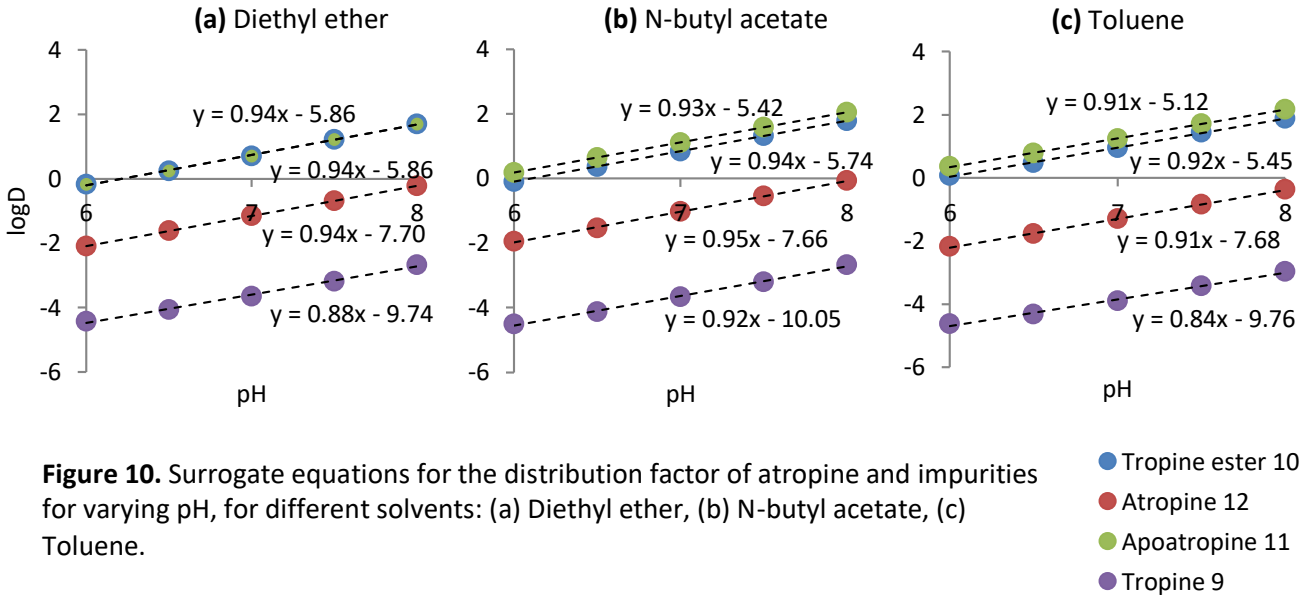

Figure 10. Surrogate equations for the distribution factor of atropine and impurities for varying pH, for different solvents: (a) Diethyl ether, (b) N-butyl acetate, (c) Toluene.

The ratio of the organic to the aqueous phase is simulated for each candidate solvent using UNIFAC, and surrogate equations are obtained by fitting polynomial or linear functions to the results.

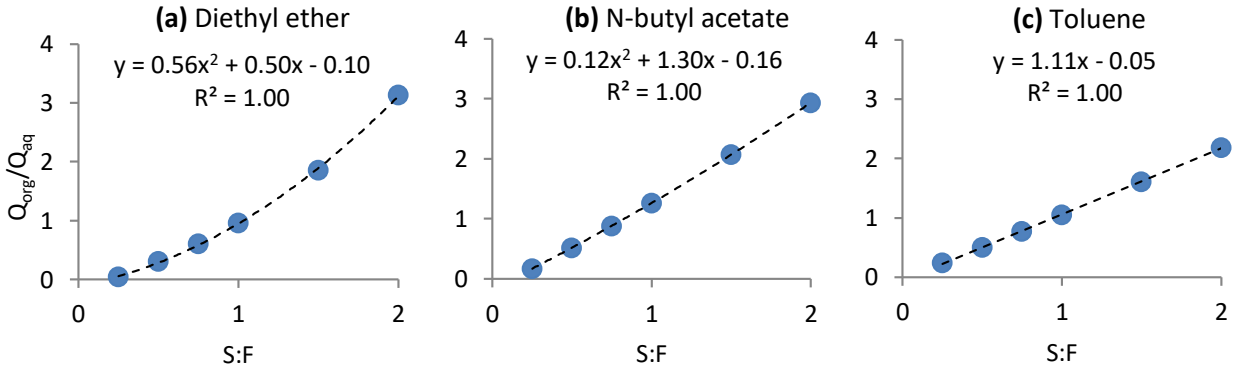

Figure 11. Surrogate equations for the ratio of the volumetric flows of the organic to the aqueous phase fitted against the solvent to feed ratio, for different extraction solvents: (a) Diethyl ether, (b) N-butyl acetate, (c) Toluene

2.4.2 Diazepam

The product stream exiting PFR II contains the API in a binary solution of toluene (98%) and MeOH (1%). The stream also contains other organic (bromoacetylchloride, intermediate amide and traces of 5-chloro-

2-(methylamino)benzophenone) and inorganic (NH3) solutes. In order to obtain pure API, impurities have to be extracted from the stream. This is done by two continuous liquid-liquid extractions.

In the first stage, water-soluble impurities (MeOH/NH_3) are removed through the addition of a polar solvent, with the API residing in the toluene-rich phase. Due to the miscibility of toluene with most available solvents, only water and some glycols produced the desired phase split. While propylene glycol is considered safe for use in pharmaceutical processes, ethylene glycol and diethylene glycol are classified as toxic materials and their use is avoided[28,29]. Thus, only water and propylene glycol are evaluated in this study.

In the second stage, organic-soluble impurities are removed by separating the API from the organic phase. This is achieved through the addition of an aqueous solution of HCl, which protonates Diazepam and allows its collection in the aqueous phase. Toluene is not miscible with the H_2O/HCl solution, so the separation of the two phases is possible through a gravitational separator.

The solubility of diazepam in the organic phase is calculated using UNIFAC, while experimental values are used for the aqueous phase. The solubility of the protonated form of diazepam in the aqueous phase is calculated using the Henderson-Hasselbalch equation[30]:

$$logS_{i,aq} = logS_{i,0} + log(1 + 10^{pKa_i - pH}) \quad (23)$$

where $S_{i,aq}$ is the solubility of the protonated form, $S_{i,0}$ is the intrinsic solubility[31] and pK_a is the acid dissociation constant[32].

The pH value of the aqueous phase is calculated by considering full dissociation of the acid:

$$pH = -log(a_{H^+} C_{H^+}) = -log(a_{H^+} C_{HCl}) \quad (24)$$

where C_{HCl} is the concentration of the solution of hydrochloric acid and a_{H^+} is the activity coefficient of protons. A surrogate equation for the proton activity coefficient as a function of the concentration of hydrochloric acid is derived from experimental data[33] and incorporated into the model.

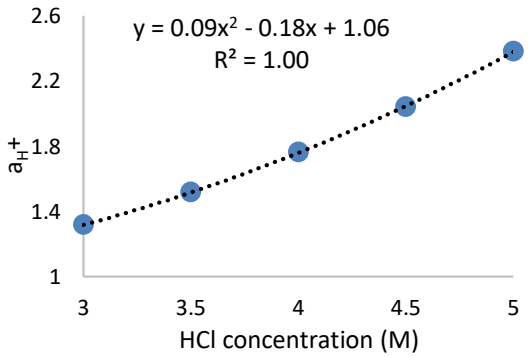

Figure 12. Determination of surrogate activity coefficient equation for varying acid concentration.

2.5 Mass transfer and LLE design

In order to calculate the actual recovery of each compound, the stage efficiency is calculated, by modelling the liquid-liquid extractor as a mixer settler:

$$E_{st} = \frac{1}{\frac{Q}{KaV_t}+1} \quad (25)$$

where Q is the volumetric flow through the tank, K is the mass-transfer coefficient, a is the liquid-liquid interfacial area and V_t is the volume of the tank.

The specific interfacial area is calculated with the assumption of spherical droplets:

$$a = \frac{6\varphi}{d_p} \quad (26)$$

where φ is the volumetric fraction of the dispersed phase and d_p is the particle diameter.

The dispersed phase volumetric fraction is calculated using the correlation of Treybal for unbaffled vessels with no vapour-liquid interface[34]:

$$\varphi = 3.39\left(\frac{PQ_d\mu_c^2}{V_t\sigma^3 g_c}\right)^{0.247}\left(\frac{\mu_c^3}{Q_d\rho_c\sigma g_c}\right)^{0.427}\left(\frac{\rho_c}{\Delta\rho}\right)^{0.430}\left(\frac{\sigma^3\rho_c g_c^3}{\mu_c^4 g}\right)^{0.401}\left(\frac{\mu_d}{\mu_c}\right)^{00987} \quad (27)$$

$$P = \frac{4\rho_m\omega^2 d_i^5}{g_c} \quad (28)$$

$$\rho_m = \varphi\rho_d + (1-\varphi)\rho_c \quad (29)$$

where subscripts d and c and denote the dispersed and continuous phase, m denotes the mixture, P is the impeller power, ω is the impeller speed, ρ is density, μ is dynamic viscosity, g is the specific gravity, σ is surface tension and Q_d is the volumetric flow of the dispersed phase. The system of equations has to be solved simultaneously.

The particle diameter d_p is calculated from the Weber number:

$$d_p = \begin{cases} 0.052 d_i We^{-0.6} e^{4\varphi} & We < 10^3 \\ 0.39 d_i We^{-0.6} & We > 10^3 \end{cases} \quad (30)$$

$$We = \frac{d_i^3\omega^2\rho_c}{\sigma} \quad (31)$$

For the calculation of K, the correlation developed by Treybal for solid particles[34] is used:

$$K = \frac{1}{\frac{1}{k_c}+\frac{1}{k_d}} \quad (32)$$

$$Sh_d = \frac{k_d d_p}{D_{i,d}} = 6.6 \quad (33)$$

$$Sh_c = \frac{k_c d_{32}}{D_{i,c}} = 2 + 0.47 \left[d_p^{\frac{4}{3}} \left(\frac{P g_c}{V_t} \right)^{\frac{1}{3}} \frac{\rho_c^{\frac{2}{3}}}{\mu_c} \right]^{0.62} \left(\frac{d_i}{d_p} \right)^{0.17} \left(\frac{\mu_c}{\rho_c D_{i,c}} \right)^{0.36} \quad (34)$$

Where k is the phase-specific mass-transfer coefficient, d_i is the impeller diameter, d_p is the particle diameter, d_t is the tank diameter, D is the diffusion coefficient.

The diffusion coefficient is calculated using the Stokes-Einstein equation:

$$D_{i,c} = \frac{k_b T}{6\pi \mu_c r_i} \quad (35)$$

$$D_{i,d} = \frac{k_b T}{6\pi \mu_d r_i} \quad (36)$$

where k_b is the Boltzmann constant and r_i is the molecular radius.

2.6 Environmental impact assessment

To quantify the environmental impact of the processes, the E-factor is used, defined as the mass of waste produced per mass of product:

$$E_{factor} = \frac{m_{waste}}{m_{API}} = \frac{m_{bpd} + m_{ur} + m_{ws} + m_{uAPI}}{m_{API}} \quad (37)$$

Where:

- bpd = byproducts
- ur = unconverted reactants
- ws = waste solvent
- $uAPI$ = unrecovered API

For the calculation of the E-factor, it is assumed that 50/70% of solvents is recycled. Water is generally excluded from the calculation, because it leads to very high E-factors[35]. However, for the evaluation of diazepam purification, the total contribution of the hydrochloric acid solution is considered (including water and hydrochloric acid), due to its acidity and the environmental hazards it poses[36].

2.7 Costing

The Free-on-Board (FOB) is calculated using a cost-capacity correlation for the equipment[37]. The Chemical Engineering Plant Cost Index (CEPCI) is used to account for inflation.

$$C_B = f C_A \left(\frac{S_B}{S_A} \right)^n \frac{CEPCI_B}{CEPCI_A} \quad (38)$$

Base costs and the parameters of the FOB correlation for each unit are given in Table 4 and Table 6 for atropine and diazepam, respectively.

The Battery Limits Installed Cost (BLIC) is calculated using the Chilton method[38]. The installed equipment cost (C_{IE}) is 1.43 times the FOB. Process piping and instrumentation (C_{PPI}) costs are 42% of C_{IE}.

The sum of C_{IE} and C_{PPI} gives the total physical plant cost (C_{TPP}), to which an engineering and construction factor of 0.3 is added, giving the BLIC.

$$C_{IE} = 1.43FOB \quad (39)$$

$$C_{PPI} = 0.42C_{IE} \quad (40)$$

$$C_{TPP} = C_{IE} + C_{PPI} \quad (41)$$

$$BLIC = 1.3C_{TPP} \quad (42)$$

Working capital costs (C_{WC}) are estimated as 3.5% of annual material cost. Contingency costs (C_{cont}) are estimated as 20% of the BLIC.

$$C_{WC} = 0.035C_{mat} \quad (43)$$

$$C_{cont} = 0.2BLIC \quad (44)$$

$$C_{WCC} = C_{WC} + C_{cont} \quad (45)$$

The capital expenditure (CapEx) is calculated as the sum of BLIC and C_{WCC}:

$$CapEx = BLIC + C_{WCC} \quad (46)$$

The materials cost (C_{mat}) is calculated as the product of the required feed mass with the corresponding purchased price. Material prices are summarised in Table 3 and Table 5 for atropine and diazepam, respectively. The cost of utilities (C_{ut}) is estimated as 0.96£/kg of material input and the cost of waste disposal (C_{wd}) is estimated as 0.35£/L of waste solvent[39] and is calculated considering the solvent recovery (SR).

$$C_{mat} = \sum_i Req_i Price_i \quad (47)$$

$$C_{util} = 0.96 \sum_i Req_i \quad (48)$$

$$C_{wd} = 0.35\ Q_{waste}(1 - SR) \quad (49)$$

The annual operational expenditure is calculated as the sum of C_{mat}, C_{util} and C_{wd}.

$$OpEx = C_{mat} + C_{util} + C_{wd} \quad (50)$$

The total cost is calculated as the sum of $CapEx$ and inflation-adjusted $OpEx$:

$$Total\ cost = \sum_{k=1}^{\tau} \frac{OpEx}{(1+i)^k} + CapEx \quad (51)$$

A lifetime (τ) of 20 years, a constant interest rate (i) of 5% and the capital expenditure happening during the first year are assumed.

2.7.1 Atropine

Table 3. Material prices for atropine synthesis and purification

Material	Price (£/kg)
Tropine	169.09
Phenylacetyl chloride	54.88
Formaldehyde	3.78
NaOH	0.27
Water	0.60
DMF	3.15
Diethyl ether	13.64
N-butyl acetate	4.32
Toluene	3.92

Table 4. Equipment cost basis for atropine synthesis and purification

Equipment type	Year	CA	f	n	Basis	SA	Units
PFR I	2014	103208	1.0106	1	mL	80	1
PFR II	2014	103208	1.0106	1	mL	80	1
LLE	2007	21000	1.1033	0.27	L	1	1
Cooler	2018	4597	-	-	L/min	21	1
Pump	2015	958	-	-	L/h	75	5

2.7.2 Diazepam

Table 5. Material prices for diazepam synthesis and purification

Material	Price (£/kg)
5-Chloro-2-(methylamino)benzo-phenone	11.70
Bromoacetylchloride	281.05
Toluene	3.92
NH3 7M in MeOH	96.39
Water	0.60
HCl aq. solution	4.13

Table 6. Equipment cost basis for diazepam synthesis and purification

Equipment type	Year	CA (£)	f	n	Basis	SA	Units
PFR I	2014	103208	1.0106	1	mL	80	1
PFR II	2014	103208	1.0106	1	mL	80	1
LLE I	2007	21000	1.1033	0.27	L	1	1
LLE II	2007	21000	1.1033	0.27	L	1	1
Cooler	2018	4597	-	-	L/min	21	2
Pump	2015	958	-	-	L/h	75	6

3 Results

3.1 Mass balances

Table 7. Mass balances for atropine synthesis and separation at key points. Capacity = 100 kg API/year.

Component	Stream (kg/yr)								
	F-103	**F-105**	**F-106**	**F-107**	**F-108**	**F-109**	**F-110**	**F-112**	**F-113**
Tropine **9**	127.6	0.0	0.0	1.3	1.3	0.0	1.3	1.2	0.1
Phenylacetyl chloride **8**	123.1	0.0	0.0	0.0	0.0	0.0	0.0	0.0	0
Ester **10**	0.0	0.0	0.0	115.2	45.1	0.0	45.1	5.5	39.6
Formaldehyde	0.0	0.0	162.7	162.7	143.5	0.0	143.5	143.5	0
Atropine **12**	0.0	0.0	0.0	0.0	112.9	0.0	112.9	100.0	12.9
Apoatropine **11**	0.0	0.0	0.0	0.0	68.1	0.0	68.1	4.5	63.6
Sodium hydroxide	0.0	43.4	0.0	43.4	7.2	0.0	7.2	7.8	0
Water	0.0	361.6	277.0	654.9	654.9	0.0	654.9	611.1	43.8
DMF	426.6	0.0	0.0	426.6	426.6	0.0	426.6	101.3	26.6
Toluene	0.0	0.0	0.0	0.0	0.0	898.0	898.0	122.0	776.0

Table 8. Mass balances for diazepam synthesis and purification at key points. Capacity = 100 kg API/year.

Component	Stream (kg/yr)								
	F-203	**F-207**	**F-208**	**F-209**	**F-210**	**F-211**	**F-212**	**F-213**	**F-214**
5-Chloro-2-(methylamino)benzophenone **1**	159.0	2.7	2.7	0.0	0.0	2.7	0.0	0.0	2.7
Bromoacetylchloride **2**	203.6	29.2	29.2	0.0	0.0	0.0	0.0	0.0	0.0
Intermediate **3**	0.0	369.9	60.1	0.0	60.1	0.0	0.0	0.0	0.0
Ammonia	0.0	77.0	69.0	0.0	53.0	16.0	0.0	1.0	15.0
Toluene	10210.0	44508.0	44508.0	0.0	4008.4	40499.6	0.0	5.2	40494.4
Methanol	0.0	435.4	435.4	0.0	334.5	100.9	0.0	94.6	6.3
Diazepam **4**	0.0	0.0	134.4	0.0	0.0	134.4	0.0	100.0	34.4
Water	0.0	0	0	20587.55	20573.65	13.9	10721.86	10708.56	13.3
Hydrochloric acid	0.0	0	0	0.0	0	0	1.8	1.8	0

3.2 PFR design

Reactors are sized based on the computed mass balances and the optimal residence times, for a plant capacity of 100 kg per annum. The reactor volumes obtained are small, which highlights the compactness of continuous pharmaceutical processes. Tube reactor lengths are calculated for various internal diameters. Typically, a large ratio of length to diameter is preferred to achieve mass and heat flow uniformity.

3.2.1 Atropine

For the first reactor, an I.D. of 3 mm is sufficient, since the rate of the reaction is high. For the second reactor a larger I.D. is more practical, due to the high residence time.

Table 9. Atropine synthesis PFR characteristics as the result of the optimization

Reactor	Residence time (min)	Conversion (%)	Volume (mL)	Internal diameter (mm)	Length (mm)
R-101	3.5	99	4.5	3	633
				6	158
				12	40
				18	18
R-102	16.2	72	45.6	3	6444
				6	1611
				12	403
				18	179

3.2.2 Diazepam

Despite the lower residence times of diazepam synthesis compared to that of atropine, the reactor volumes computed are larger. This is due to the high mass throughput of the process, and the use of I.D. larger than 3 mm is suggested to avoid excessively lengthy reactors.

Table 10. Diazepam synthesis PFR characteristics as the result of the optimization

Reactor	Residence time (min)	Conversion (%)	Volume (mL)	Internal diameter (mm)	Length (mm)
R-201	1	98	26.8	3	3794
				6	949
				12	237
				18	105
R-202	0.64	74	69.5	3	9834
				6	2458
				12	615
				18	273

3.3 LLE design

3.3.1 Atropine

Having pure organic and aqueous phases is highly desirable, since it results in better partitioning between water soluble and water in-soluble compounds, while also ensuring the validity of the theoretical distribution factors, calculated for pure solvents, which are used for mixed solvents in this study.

The molar fraction of DMF in each phase is less than 15%, which is considered low enough, especially when translated into volume fraction. With the use toluene, it is possible to generate two virtually binary phases (toluene-DMF, water-DMF), due to the high immiscibility between water and toluene. Diethyl ether and n-butyl acetate yield less pure streams.

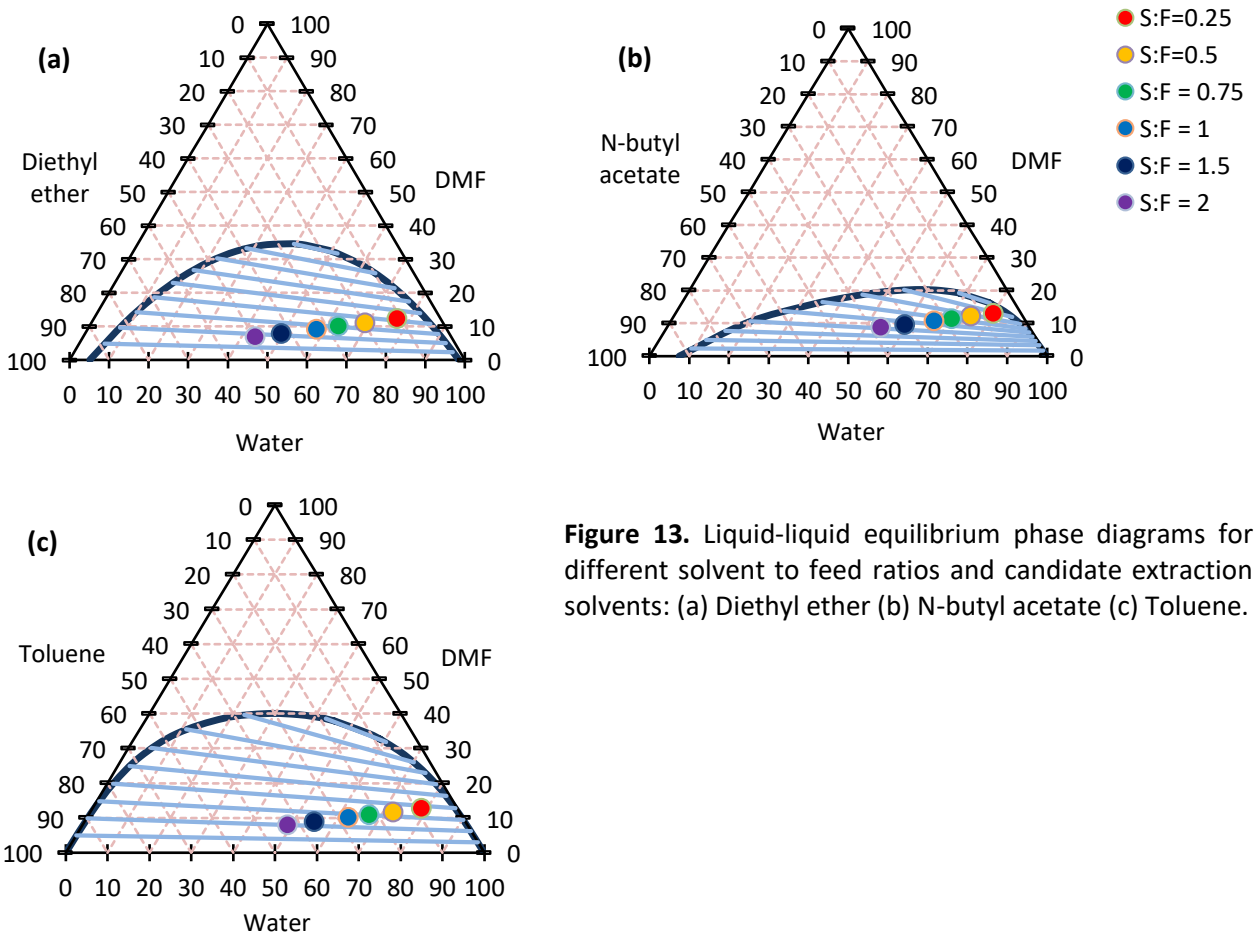

Figure 13. Liquid-liquid equilibrium phase diagrams for different solvent to feed ratios and candidate extraction solvents: (a) Diethyl ether (b) N-butyl acetate (c) Toluene.

Figure 14 shows that the recovery for all compounds decreases with increasing pH, while purity generally increases. Although the concentration of tropine **9** in the product stream is not significant, the recovery of the API in the aqueous phase for high pH values is so small that the concentration of tropine

9 becomes of the same magnitude with that of atropine **12**, and the purity decreases. This is also the reason that the oscillations of purity become more imminent at high pH values. The optimum pH for the operation of the LLE is between the maximum of the recovery and the maximum of the purity, which is for pH = 6-8.

Toluene performs the best in terms of recovery, while also achieving the highest purity (97%) among the three candidate solvents. This result is attributed to both the phase equilibrium properties of the system water-DMF-toluene and the properties of toluene as solvent. With water being virtually absent from the organic stream, the aqueous stream is bigger in volume, which yields a high API recovery. In addition, the distribution coefficient of atropine for pH>6 is low in toluene, which results in more API residing in the aqueous phase. Diethyl ether has lower distribution coefficients values, but also yields smaller volume aqueous streams for high solvent to feed ratios, thus resulting in decreased recovery. As a result, diethyl ether performs well only at low solvent to feed ratios.

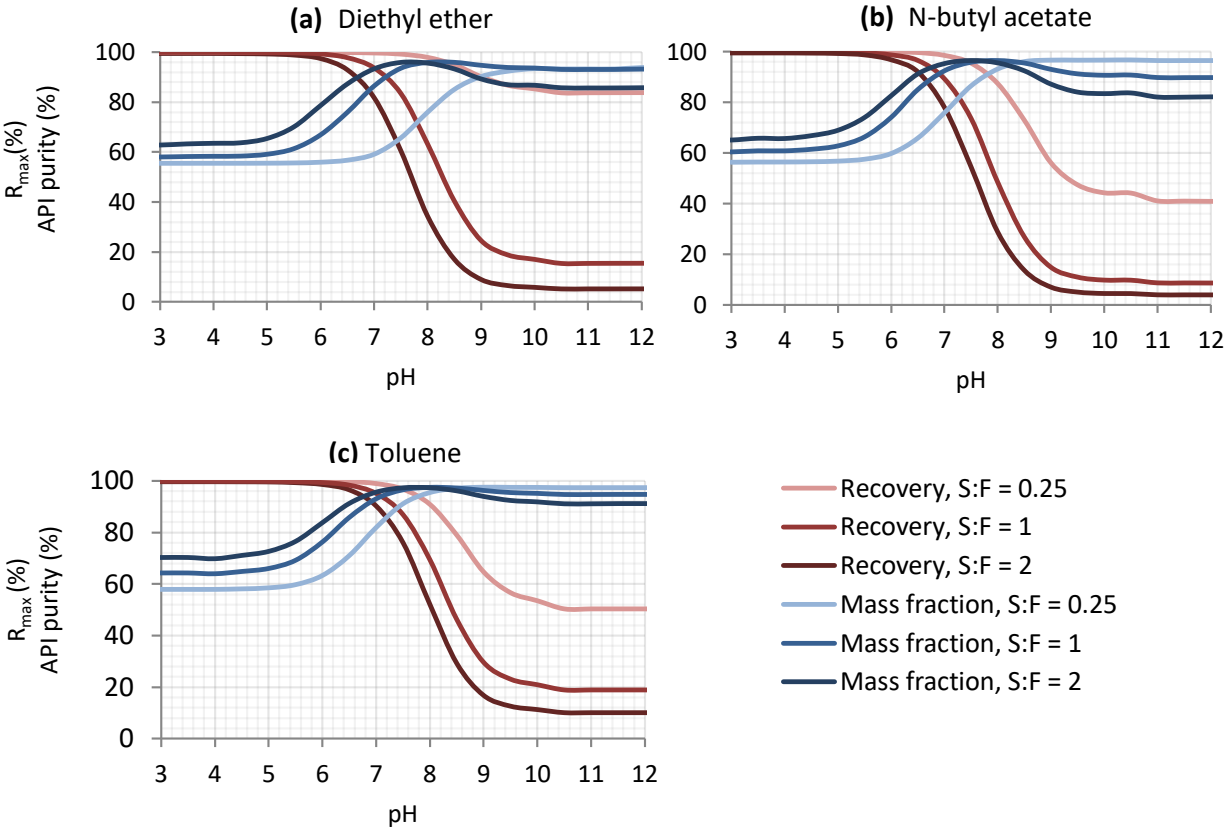

Figure 14. Theoretical API recovery in the aqueous phase and API purity (% mass) for different pH values, solvent to feed ratios and extraction solvents: (a) Diethyl ether (b) N-butyl acetate (c) Toluene.

Figure 15 shows that the behavior of stage efficiency is similar for all solvents, with the optimal solvent to feed ratio being close to 0.5. The solvents decrease in efficiency with increasing surface tension and viscosity, which explains the higher efficiency exhibited by diethyl ether, followed by toluene, and n-butyl acetate last. For adequate residence times, high efficiency (90%) is achieved for all cases.

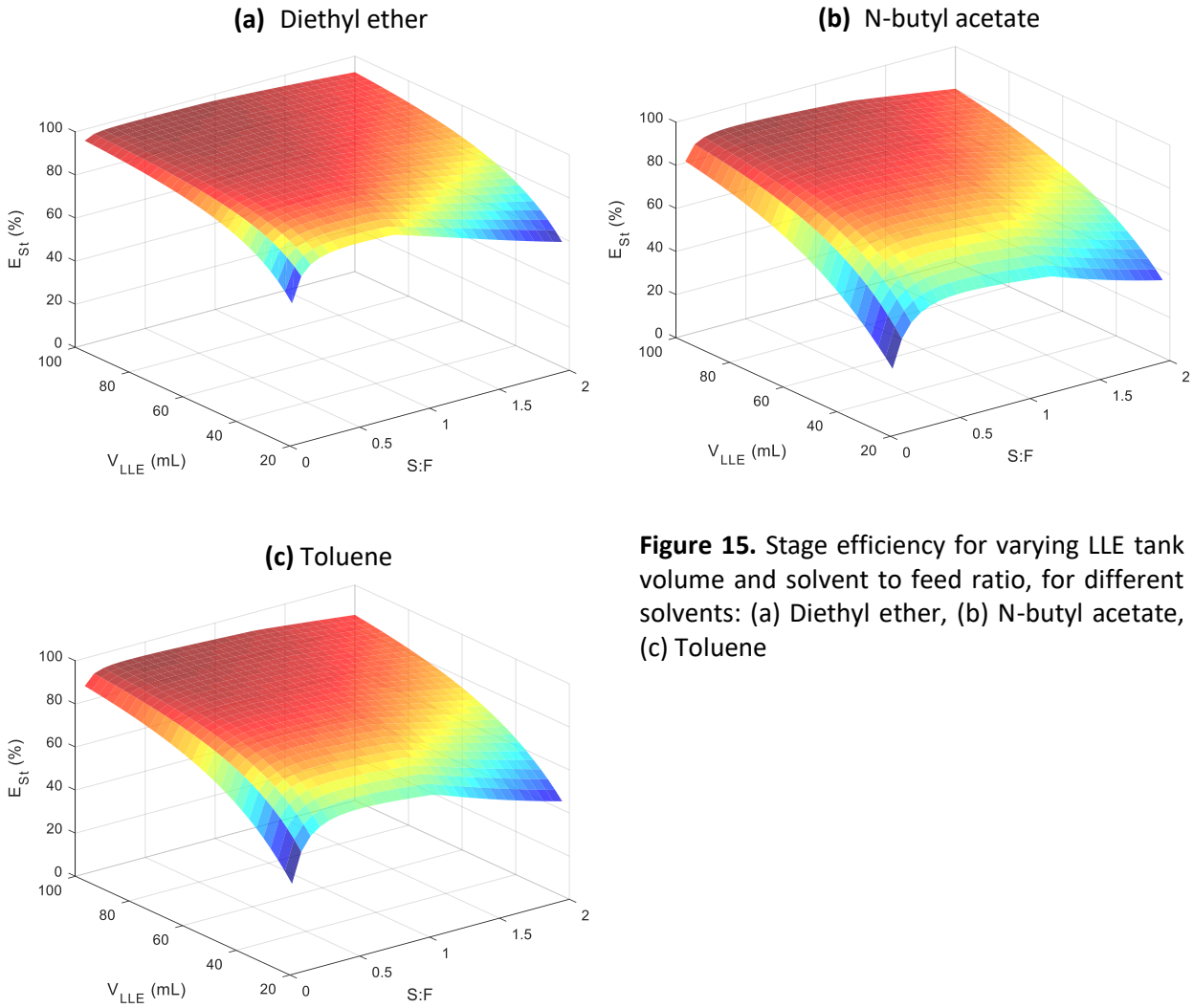

Figure 15. Stage efficiency for varying LLE tank volume and solvent to feed ratio, for different solvents: (a) Diethyl ether, (b) N-butyl acetate, (c) Toluene

3.3.2 Diazepam

The performance of the first separation decreases with increasing temperature, as the binodal curve becomes smaller, thus resulting in less pure phases. This happens due to the miscibility between the organic compounds (methanol-toluene when using water, methanol-toluene-propylene glycol when using propylene glycol) increasing with temperature.

When using water as solvent, it is possible to generate two virtually binary phases; an organic phase, rich in toluene with small amounts of water, and an aqueous phase containing methanol. Toluene and water are immiscible, so the amount of waste toluene containing the API in the aqueous phase is negligible, given the conditions of the feed. When using propylene glycol as extraction solvent, the composition of the waste stream is a ternary mixture of the solvent, methanol and toluene. The composition of the waste stream suggests that it will contain dissolved API. The organic stream does not contain any propylene glycol, which would complicate subsequent separations.

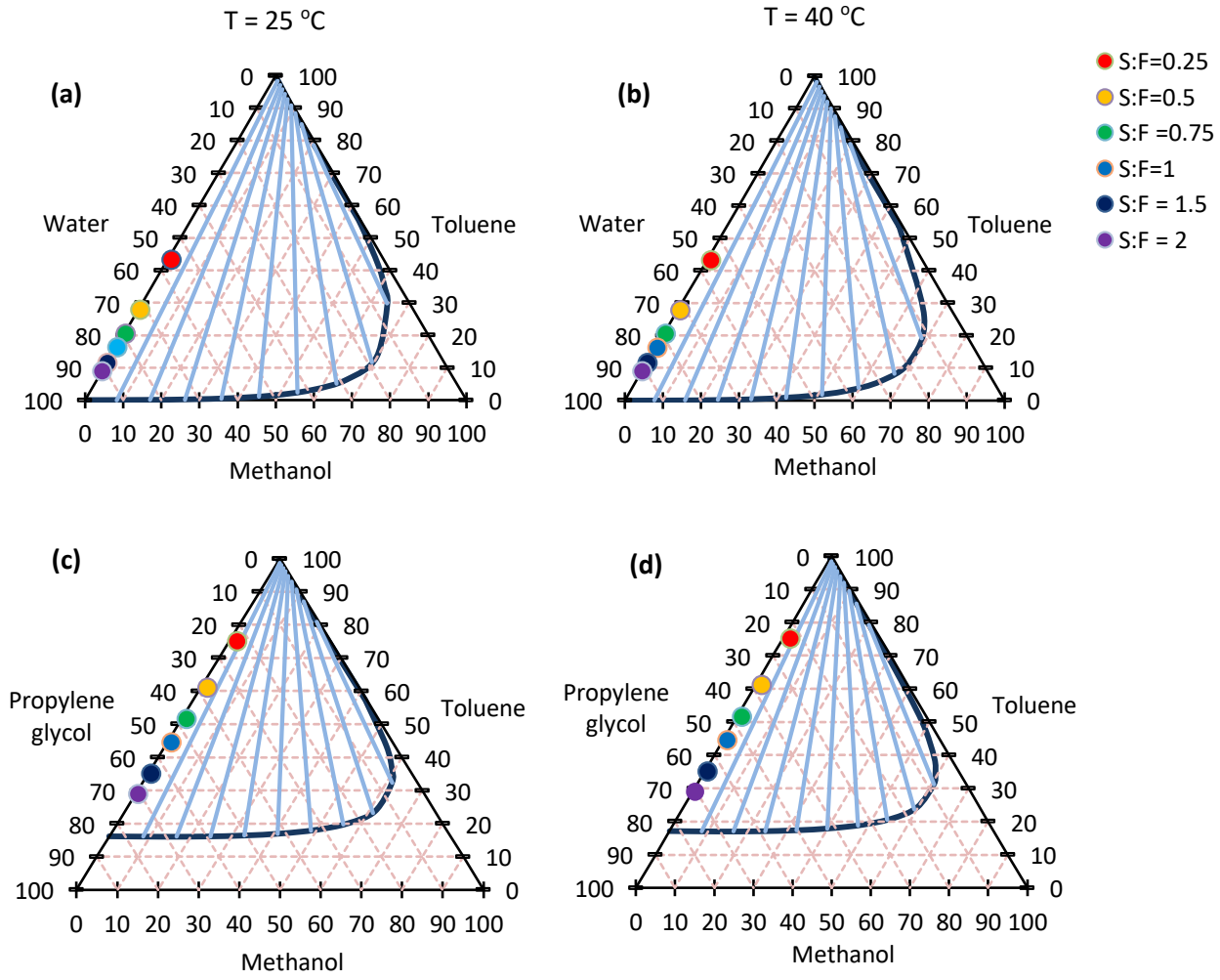

Figure 16. Liquid-liquid equilibrium phase diagrams for two temperatures (25, 40 °C) and candidate extraction solvents: (a) Water, (b) Propylene glycol.

For the separation of water-soluble impurities, Figure 17 shows that by increasing the solvent to feed ratio, the percentage of methanol removed from the organic stream increases. For water, the theoretical recovery is higher than propylene glycol, but this difference becomes less accented at higher ratios.

Due to the very low miscibility between toluene and water, the amount of toluene with dissolved API being transferred to the aqueous phase is negligible. In addition, due to low solubility of the API in the aqueous phase, the amount of API being transferred to the aqueous phase is also negligible. Thus, 100% of the API will reside in the organic stream after the first separation when using water as solvent.

When using propylene glycol, there is a significant amount of API residing in the waste stream, which results in lower recovery. The recovery further decreases with increasing solvent to feed ratio, due to the volume of the waste stream increasing. Water presents overall better performance than propylene glycol and has no toxicity. Since propylene glycol does not present any benefits, water is considered as the only extraction solvent for the separation of water-soluble impurities.

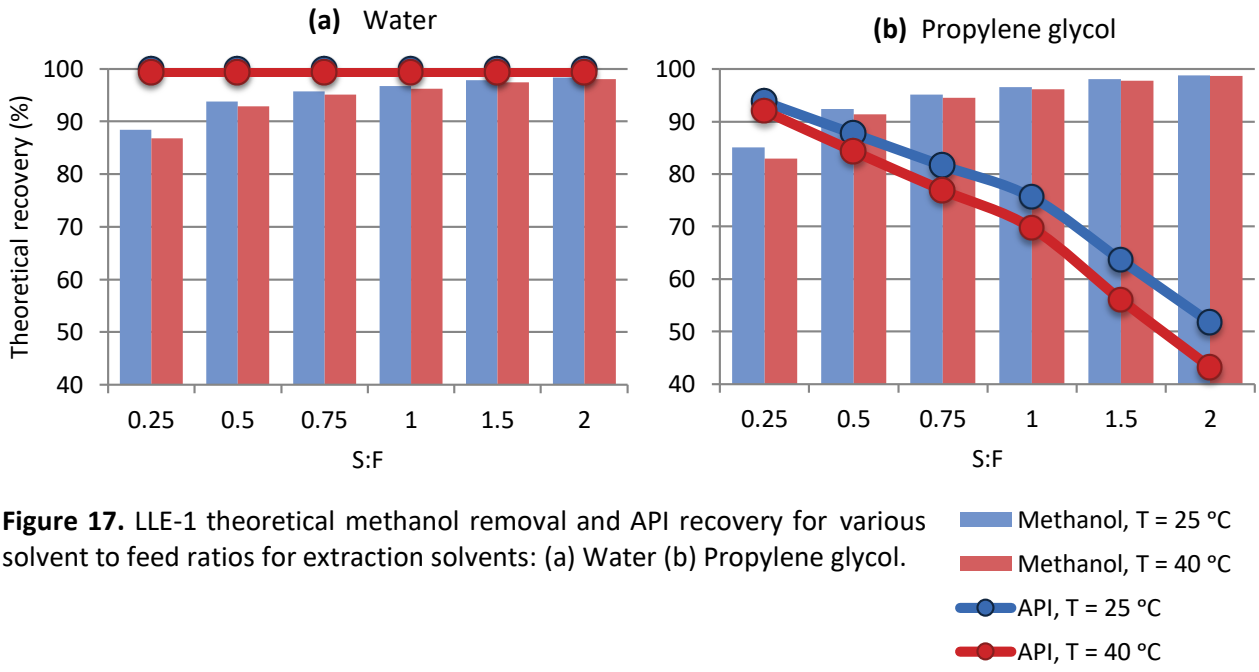

Figure 17. LLE-1 theoretical methanol removal and API recovery for various solvent to feed ratios for extraction solvents: (a) Water (b) Propylene glycol.

For the separation of water-insoluble impurities, there is inevitable loss of API to the organic stream, which is the waste stream. As shown in Figure 18, the recovery of the API in the aqueous stream increases with both increasing solvent to feed ratio and acid solution concentration. The latter is expected by the Henderson-Hasselbalch equation, which predicts that the solubility of the cation of the API in water is higher for lower pH values.

It can be seen that for low solvent to feed ratios, strongly acidic conditions are required for a decent API recovery, while for higher solvent to feed ratios the effect of the pH becomes less significant. The ability to operate at more moderate pH conditions is highly desirable.

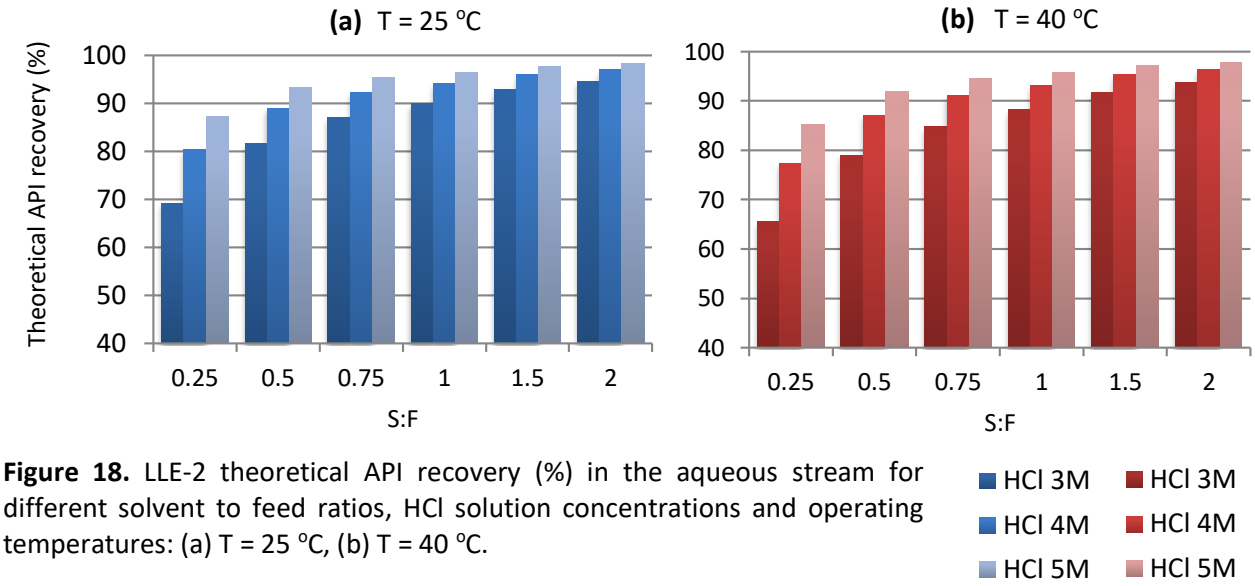

Figure 18. LLE-2 theoretical API recovery (%) in the aqueous stream for different solvent to feed ratios, HCl solution concentrations and operating temperatures: (a) T = 25 °C, (b) T = 40 °C.

In Figure 19, the first efficiency diagram depicts the transfer of methanol from the organic into the aqueous stream, while the second diagram depicts the transfer of atropine from the organic into the aqueous stream. The efficiency of the first separation is higher. This is expected, since methanol is a smaller molecule than diazepam, which facilitates the diffusion. Again, the optimal solvent to feed ratio is around 0.5 and the efficiencies are high for all cases for adequate residence times.

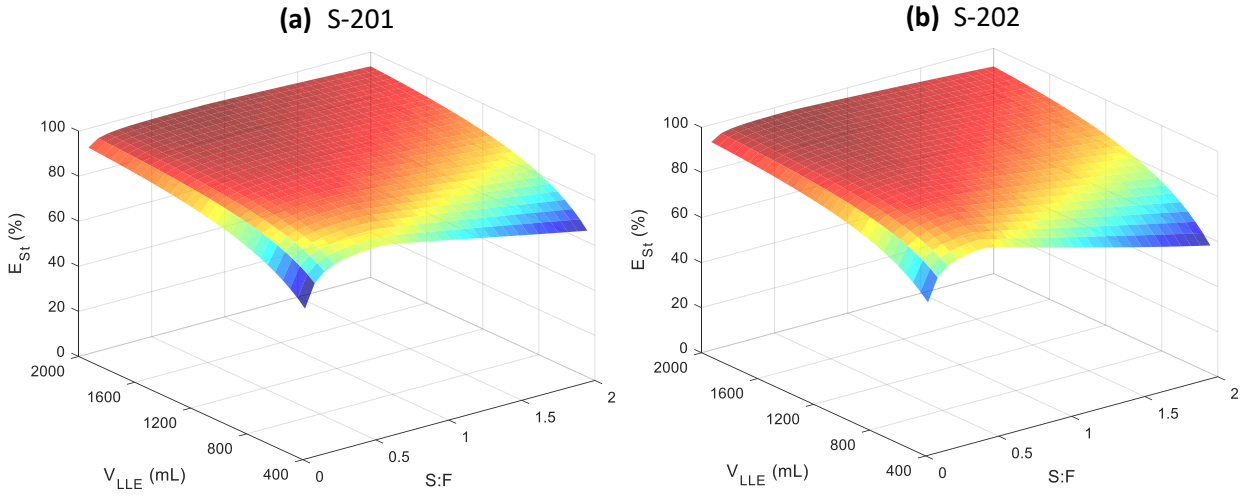

Figure 19. Stage efficiency for varying LLE tank volume and solvent to feed ratio, for the two separations: (a) S-201 (using water), (b) S-202

3.4 Economic and environmental analysis

The two processes are modelled and optimised with respect to several design variables: reactor volumes, separator volumes, solvent to feed ratios and separation pH values. The non-linear optimisation problem is solved for each API for two solvent recovery cases (50% and 70%), by minimising the total cost. The problem is formulated on MATLAB and solved using the interior point algorithm. For the atropine process, two different product purities are considered, implemented as constraints to the problem. For the diazepam process, two different separation temperatures are considered.

There is a trade-off between conversion and reactor size, as large residence times tend to increase the CapEx due to larger capacities and low residence times tend to increase the OpEx due to higher material input requirements. The solution is sensitive to material prices, especially for those materials with high throuhput, such as sovlents. CapEx and Opex are closely associated with API recovery in the separation process, as a decrease in recovery leads to an increase in materials and reactor dimensions. Maximum recovery is always desired in the separation stage, as the cost of the liquid-liquid extraction unit is insignificant.

3.4.1 Atropine

The minimal total cost achieved for 70% solvent recovery is 6.40×10^5 GBP for 90% purity and 6.76×10^5 GBP for 95% purity, and it corresponds to the use of toluene as extraction solvent. High purity is desirable, as it minimises the downstream processing requirements. When higher purity is demanded, both the total cost and the E-factor increase, due to the recovery decreasing.

The cost effectiveness of toluene is expected, as it exhibits high API recovery, while also having the lowest price among the three solvents. Having a higher price but better extraction performance, diethyl ether has a higher cost than toluene but lower than that of n-butyl acetate for the low purity case. However, the cost of diethyl ether is the highest among the three solvents for the high purity case. This is a result of the imposed purity constraint, which drives the recovery at lower values.

The lowest E-factor is achieved when using diethyl ether (6.8) for low purity, followed by toluene and n-butyl acetate. This result better reflects that diethyl ether is the most efficient solvent with a soft purity constraint. Again, diethyl ether is characterised by the highest E-factors for the high purity case, followed by n-butyl acetate and toluene.

For 70% solvent recovery, the optimal reactor residence time ranges between 16 to 19 minutes, being slightly higher for high purity, to reduce the mass of the unreacted reagents in the product stream. The optimal solvent to feed ratio ranges between 0.4 and 0.8. The optimal pH is limited to basic values by the purity constraint, and it increases with increasing purity. It is worth noting that for the lowest cost case, the optimal pH is found to be 7, which means that the separation can take place in neutral conditions and may not require further pH adjustment other than a neutralisation.

The same trend is followed when 50% solvent recovery is assumed. Since the OpEx constitutes most of the total cost, all of the problems converge to solutions that are characterised by high separation API recovery. However, for 50% solvent recovery, the problem converges to higher residence times for the reactors, often bound-limited, in order to increase the yield and reduce the total mass input of the

process. The OpEx compromises a larger portion of the total cost, due the increased material cost, while the CapEx is not remarkably increased.

The E-factors achieved are small, in the range of fine chemicals. This is due to the use of concentrated streams throughout the process and the assumed partial recovery of the carrier and extraction solvents. However, another important criterion for solvent selection is its toxicity. N-butyl acetate is the less toxic solvent of the three, listed as Class 3 solvent by the FDA, meaning it poses no known risks to human health. Toluene and diethyl ether are both listed as Class 2 solvents due to their inherent toxicity and their use should be limited in pharmaceutical products[40]. Especially the use of diethyl ether is avoided due to its high volatility and low flash point (-45 ^{o}C).

3.4.2 Diazepam

The minimal total cost achieved for 70% solvent recovery is 33.7×10^5 GBP with the use of 5M HCl solution, at 25 ^{o}C. The total cost increases with decreasing acid solution concentration, due to the API recovery of the separation decreasing. The recovery decreases with increasing temperature due to the solubility of the API increasing more for the organic phase compared to the aqueous phase, as calculated by the UNIFAC model. The effect of temperature is not very significant, so the operation of the two LLE units at 40 ^{o}C is preferred to avoid cooling the effluent of the second reactor to ambient temperature. E-factors follow the same trend as the total cost, with the minimal E-factor being 146 (148 for the high temperature case).

For all cases, both reactors' residence times are driven to the higher bounds (1, 0.64 minutes) and the optimal solvent to feed ratio is between 0.25 and 0.4). The influence of the solvent to feed ratio to the cost is more detrimental for the case of 50% solvent recovery; the value is increased, to allow for higher API recovery and reduce the carrier solvent throughput, while for 70% solvent recovery there is a trade-off between carrier and extraction solvent cost.

Both the E-factor and the total cost drastically increased in the case of 50% solvent recovery, due to higher material input requirements. Interestingly, although the OpEx is increased, the CapEx appears to be slightly smaller compared to the case of 70% solvent recovery. This is a result of the higher API recovery achieved by the higher solvent to feed ratio, resulting in smaller mass throughput.

The observed E-factors for diazepam are very high, even for pharmaceutical processes, and that is due to the low solubility of diazepam in the feed stream of the second reactor, in presence of ammonia/methanol. The suggested dilution of 1:4 requires excessive amounts of carrier solvent, which also leads to a high requirement of extraction solvents in the subsequent separation steps.

The excessive use of carrier solvent during the synthesis of diazepam is reflected on both the OpEx and the E-factor. The OpEx is a magnitude of order higher than the CapEx, which is due to the increased material throughput, while around 20% of the OpEx is constituted of waste handling costs. Given the low concentration of solutes in toluene, a higher percentage of solvent recovery would not be unrealistic.

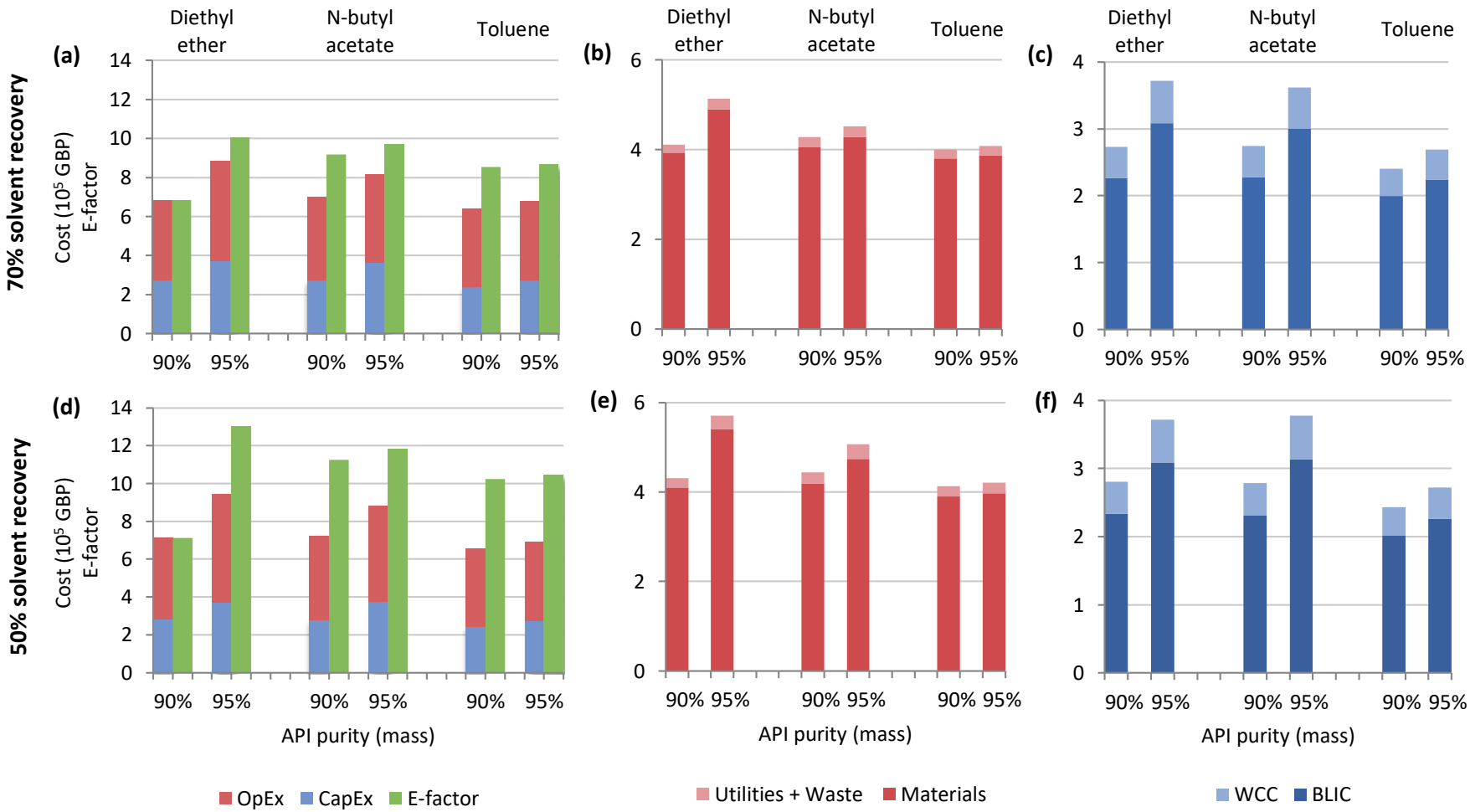

Figure 20. Optimisation results for two API purities and three extraction solvents. Minimisation of total cost: (a) Total cost, E-factor, (b) OpEx, (c) CapEx. Minimisation of E-factor: (d) Total cost, E-factor, (e) OpEx, (f) CapEx.

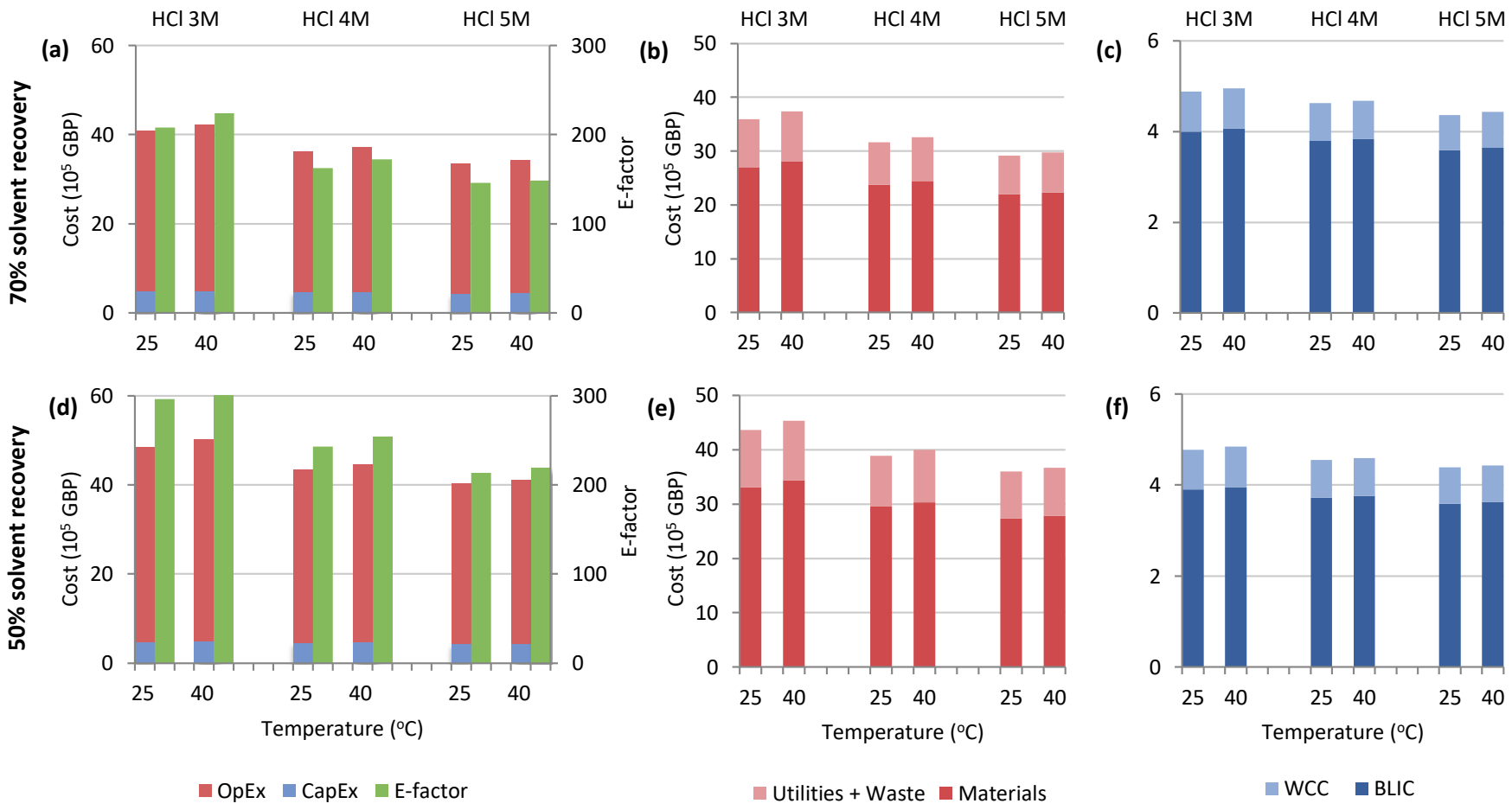

Figure 21. Optimisation results for two LLE-2 operating temperatures and three HCl solution concentrations. Minimisation of total cost: (a) Total cost, E-factor, (b) OpEx, (c) CapEx. Minimisation of E-factor: (d) Total cost, E-factor, (e) OpEx, (f) CapEx.

4 Discussion

4.1 Limitations of the current work

The current work is based on several key assumptions. For the separation process of atropine, the equilibrium calculations for the API during the separation stage are limited by the available computationally derived distribution factors, which correspond to pure solvent-water systems. As a simplification, mono-component streams are considered during the separation, which introduces errors on both on API recovery and purity. The results presented for atropine are optimistic, and the accuracy of the assumptions decreases in the following order: toluene, diethyl ether, n-butyl acetate. In addition, it is not clarified to which temperature the distribution factors provided correspond to, so a temperature of 25 ^{o}C is assumed. With the exception of diethyl ether, no distribution factors are calculated at higher temperatures for other solvents, which prevents the evaluation of higher temperatures for the LLE.

For diazepam, the synthesis conditions studied by Ewan et al. were only optimised with respect to product yield, without taking into consideration environmental metrics. The solubility issues are introduced before the second reactor by the addition of ammonia/methanol and result in excessive solvent use. The existence of electrolytes does not allow the solubility evaluation at this stage using the traditional UNIFAC method, so stream heating or solvent removal before the LLE could not be evaluated. It is worth noting that Bédard et al. overcome the solubility issues, but unfortunately, their experiments do not provide sufficient data for the derivation of reaction kinetics for these conditions.

For the separation process of diazepam, there was lack of UNIFAC LLE parameters for two of the functional groups of the API. VLE parameters were used instead for those two groups, which introduces error in the solubility of the API in the organic phase. Also, the liquid-liquid parameters of UNIFAC have been fitted to temperatures between 10 ^{o}C and 40 ^{o}C, so the evaluation of API solubility at higher temperatures is not possible and the LLE is only evaluated for 25 ^{o}C and 40 ^{o}C.

The material prices used in this study, which are taken from various vendors, are relatively higher than previous studies. This can result in over-estimation of the material cost, and consequently of the OpEx. On the other side, while the scaled costing of the reactors is conservative, the costing of the liquid-liquid extraction units is scaled down from a much larger basis than those used in CPM. This can result in underestimation of the CapEx, and leads to solutions which if unconstrained, are characterised by unreasonably high residence times for the separation process.

Finally, there is comparison to the equivalent batch processes for the production of atropine and diazepam, due to lack of data.

4.2 Future work

In order to fully elucidate the benefits of CPM, it is essential to project the cost savings against the batch method. Although this study is quite conclusive about the feasibility of each process, it would be purposeful to model and cost the synthesis and separation of atropine and diazepam for the current methods of production, in order to highlight the differences in equipment size, cost and environmental impact.

In addition, the current model can be improved by more accurate thermodynamic simulations. For atropine, distribution factors need to be calculated for mixed solvent streams. More extractions solvents could also be considered, apart from the three studied here. For diazepam, it is important to investigate the possibility of carrier solvent evaporation, in order to reduce the mass of extraction solvent during the LLE stages.

A much more significant improvement to the solvent use of diazepam can be achieved by changing the synthesis conditions. Bédard et al. have suggested a method which has experimentally proved to reduce the E-factor of the process to 9. It includes the use of NMP as carrier solvent, the addition of ammonium hydroxide as a source of ammonia, the mixing with an aqueous stream and the heating at 60 ^{o}C. Compilation of continuous flow chemistry data under these conditions is essential for a new flowsheet model to be developed.

The current model can also be expanded, to include continuous crystallisation of the two APIs from the aqueous stream, and downstream processing, such as tablet formation. An end-to-end, material to final product demonstration for atropine and diazepam could show even more explicitly the advantages of CPM.

4.3 Conclusion

A flowsheet steady-state model is developed for the CPM of atropine and diazepam, in order evaluate its technical, economic and environmental feasibility. The continuous chemistry relies on published work by Bédard for atropine and Ewan for diazepam, and includes novel kinetic expressions. The separations are modeled using both experimental data and simulations, which are incorporated as surrogate equations. The complexity of the systems required several assumptions to be made. Reactor residence time, extraction solvent to feed ratio and extraction pH are all important design variables for the optimisation. The results show the CPM of atropine to be very efficient, thanks to the concentrated/neat streams used. The selectivity of the extraction process achieves high purity and minimises the need for further purification. The CPM of diazepam under the conditions studied is non-efficient, since its low solubility results in excessive solvent use, which translates into high OpEx and E-factor. However, there are studies showcasing alternative methods which can be explored.

5 Nomenclature

Latin	
a	Specific interfacial area (m^2)
a_{H^+}	Proton activity coefficient
$BLIC$	Battery limits installed cost (£)
$CapEx$	Capital expenditure (£)
C_A	Cost of equipment (£)
C_B	Basis cost of equipment (£)
$C_{i,0}$	Initial concentration of compound i (mol L^{-1})
$C_{i,p}$	Concentration of compound i in phase p (mol L^{-1})
C_{cont}	Contingency cost (£)
$CEPCI$	Chemical Engineering Plant Cost Index

C_{IE}	Installed equipment cost (£)
C_{mat}	Materials cost (£)
C_{PPI}	Process piping and instrumentation cost (£)
C_{WC}	Working capital cost (£)
C_{WCC}	Working capital and contingency cost (£)
C_{wd}	Waste disposal cost (£)
C_{util}	Utilities cost (£)
D	Diffusion coefficient ($m^2\ s^{-1}$)
D_i	Distribution factor of component i
d_j	Diameter (m)
$E-factor$	Environmental factor
E_{sT}	Stage efficiency
f	Equipment cost correction factor
FOB	Free-on-board cost (£)
g	Specific gravity
i	Interest rate
K	Total mass transfer coefficient ($m\ s^{-1}$)
K_{eq}	Equilibrium constant
k_p	Phase specific mass transfer coefficient ($m\ s^{-1}$)
k_{102}	First-order reaction constant (min^{-1})
k_{201}	Second-order reaction constant ($L\ mol^{-1}\ min^{-1}$)
k_{202}	First-order reaction constant (min^{-1})
$\dot{m}_i$	Mass flow of compound i ($kg\ yr^{-1}$)
n	Equipment cost exponent
$OpEx$	Operational expenditure (£)
P	Impeller power ($J\ s^{-1}$)
pK_a	Acid dissociation constant
$Price_i$	Price of material i (£ kg^{-1})
r_i	Rate of consumption of compound i
$R_{max,i,aq}$	Maximum (theoretical) recovery of compound i in the aqueous phase
Req_i	Mass requirement for material i ($kg\ yr^{-1}$)
S_h	Sherwood number
S_i	Capacity of equipment
$S_{i,p}$	Solubility of compound i in phase p ($mol\ L^{-1}$)
$S{:}F$	Solvent to feed ratio
V	Volume (m^3)
We	Weber number

Greek

μ_i	Dynamic viscosity of i ($N\ s\ m^{-2}$)
ρ_i	Density of component i ($kg\ m^{-3}$)
σ_i	Surface tension ($N\ m^{-1}$)
τ	Residence time (min)
φ	Volumetric fraction of the dispersed phase

6 References

[1]S. Neuman, "Pharmaceutical industry wastes $50 billion a year due to inefficient manufacturing | The Source | Washington University in St. Louis", *The Source*, 2006. [Online]. Available: https://source.wustl.edu/2006/10/pharmaceutical-industry-wastes-50-billion-a-year-due-to-inefficient-manufacturing/.

[2]L. Ramsey, "We're running out of commonly used drugs — and hospitals say it's 'quickly becoming a crisis'", *Business Insider*, 2017. [Online]. Available: http://uk.businessinsider.com/drug-shortages-are-getting-worse-american-hospital-association-2017-11?r=US&IR=T.

[3]J. DiMasi, H. Grabowski and R. Hansen, "Innovation in the pharmaceutical industry: New estimates of R&D costs", *Journal of Health Economics*, vol. 47, pp. 20-33, 2016.

[4]A. Martin, A. Siamaki, K. Belecki and B. Gupton, "A flow-based synthesis of telmisartan", *Journal of Flow Chemistry*, vol. 5, no. 3, pp. 145-147, 2015.

[5]N. Suveges, R. de Souza, B. Gutmann and C. Kappe, "Synthesis of Mepivacaine and Its Analogues by a Continuous-Flow Tandem Hydrogenation/Reductive Amination Strategy", *European Journal of Organic Chemistry*, vol. 2017, no. 44, pp. 6511-6517, 2017.

[6]T. Tetsu, H. Oyamada and S. Kobayashi, "ChemInform Abstract: Multistep Continuous-Flow Synthesis of (R)- and (S)-Rolipram Using Heterogeneous Catalysts.", *ChemInform*, vol. 46, no. 29, p. no-no, 2015.

[7]S. Marre, A. Adamo, S. Basak, C. Aymonier and K. Jensen, "Design and Packaging of Microreactors for High Pressure and High Temperature Applications", *Industrial & Engineering Chemistry Research*, vol. 49, no. 22, pp. 11310-11320, 2010.

[8]M. Movsisyan, E. Delbeke, J. Berton, C. Battilocchio, S. Ley and C. Stevens, "ChemInform Abstract: Taming Hazardous Chemistry by Continuous Flow Technology", *ChemInform*, vol. 47, no. 44, 2016.

[9]A. Bogdan, S. Poe, D. Kubis, S. Broadwater and D. McQuade, "The Continuous-Flow Synthesis of Ibuprofen", *Angewandte Chemie International Edition*, vol. 48, no. 45, pp. 8547-8550, 2009.

[10]S. Mascia, P. Heider, H. Zhang, R. Lakerveld, B. Benyahia, P. Barton, R. Braatz, C. Cooney, J. Evans, T. Jamison, K. Jensen, A. Myerson and B. Trout, "End-to-End Continuous Manufacturing of Pharmaceuticals: Integrated Synthesis, Purification, and Final Dosage Formation", *Angewandte Chemie*, vol. 125, no. 47, pp. 12585-12589, 2013.

[11]A. Adamo, R. Beingessner, M. Behnam, J. Chen, T. Jamison, K. Jensen, J. Monbaliu, A. Myerson, E. Revalor, D. Snead, T. Stelzer, N. Weeranoppanant, S. Wong and P. Zhang, "On-demand continuous-flow production of pharmaceuticals in a compact, reconfigurable system", *Science*, vol. 352, no. 6281, pp. 61-67, 2016.

[12]F. Agostino and S. Krylov, "Advances in steady-state continuous-flow purification by small-scale free-flow electrophoresis", *TrAC Trends in Analytical Chemistry*, vol. 72, pp. 68-79, 2015.

[13]M. Sen, A. Chaudhury, R. Singh, J. John and R. Ramachandran, "Multi-scale flowsheet simulation of an integrated continuous purification–downstream pharmaceutical manufacturing process", *International Journal of Pharmaceutics*, vol. 445, no. 1-2, pp. 29-38, 2013.

[14]G. Macdonald, "Janssen working on other continuous processes post US FDA OK for Prezista", *in-pharmatechnologist.com*, 2016. [Online]. Available: https://www.in-pharmatechnologist.com/Article/2016/04/13/Janssen-working-on-other-continuous-processes-post-US-FDA-OK-for-Prezista. [Accessed: 14- May- 2018].

[15]H. Jolliffe and D. Gerogiorgis, "Process modelling and simulation for continuous pharmaceutical manufacturing of ibuprofen", *Chemical Engineering Research and Design*, vol. 97, pp. 175-191, 2015.

[16]B. Benyahia, R. Lakerveld and P. Barton, "A Plant-Wide Dynamic Model of a Continuous Pharmaceutical Process", *Industrial & Engineering Chemistry Research*, vol. 51, no. 47, pp. 15393-15412, 2012.

[17]Z. Wang, M. Escotet-Espinoza and M. Ierapetritou, "Process analysis and optimization of continuous pharmaceutical manufacturing using flowsheet models", *Computers & Chemical Engineering*, vol. 107, pp. 77-91, 2017.

[18]E. MacLaren, "Valium History and Statistics - DrugAbuse.com", *DrugAbuse.com*, 2016. [Online]. Available: https://drugabuse.com/library/valium-history-and-statistics/. [Accessed: 14- May- 2018].

[19]A. Bédard, A. Longstreet, J. Britton, Y. Wang, H. Moriguchi, R. Hicklin, W. Green and T. Jamison, "Minimizing E-factor in the continuous-flow synthesis of diazepam and atropine", *Bioorganic & Medicinal Chemistry*, vol. 25, no. 23, pp. 6233-6241, 2017.

[20]H. Ewan, K. Iyer, S. Hyun, M. Wleklinski, R. Cooks and D. Thompson, "Multistep Flow Synthesis of Diazepam Guided by Droplet-Accelerated Reaction Screening with Mechanistic Insights from Rapid Mass Spectrometry Analysis", *Organic Process Research & Development*, vol. 21, no. 10, pp. 1566-1570, 2017.

[21]C. Dai, D. Snead, P. Zhang and T. Jamison, "Continuous-flow synthesis and purification of atropine with sequential in-line separations of structurally similar impurities", *Journal of Flow Chemistry*, vol. 5, no. 3, pp. 133-138, 2015.

[22]J. Clayden, N. Greeves and S. Warren, Organic chemistry, 2nd ed. Oxford: Oxford University Press, 2012, pp. 689-720.

[23]W. Lund, T. Waaler, V. Meisalo and P. Kelly, "The Kinetics of Atropine and Apoatropine in Aqueous Solutions.", Acta Chemica Scandinavica, vol. 22, pp. 3085-3097, 1968.

[24]G. Hendriks, D. Uges and J. Franke, "Reconsideration of sample pH adjustment in bioanalytical liquid–liquid extraction of ionisable compounds", Journal of Chromatography B, vol. 853, no. 1-2, pp. 234-241, 2007.

[25]L. Briggner, R. Hendrickx, L. Kloo, J. Rosdahl and P. Svensson, "Solid-State Perturbation for Solubility Improvement: A Proof of Concept", ChemMedChem, vol. 6, no. 1, pp. 60-62, 2010.

[26]D. Perrin, B. Dempsey and E. Serjeant, PKa prediction for organic acids and bases. p. 9.

[27]K. Sarmini and E. Kenndler, "Ionization constants of weak acids and bases in organic solvents", Journal of Biochemical and Biophysical Methods, vol. 38, no. 2, pp. 123-137, 1999.

[28]J. Brent, "Current Management of Ethylene Glycol Poisoning", Drugs, vol. 61, pp. 979-988, 2001.

[29]L. Schep, R. Slaughter, W. Temple and D. Beasley, "Diethylene glycol poisoning", Clinical Toxicology, vol. 47, no. 6, pp. 525-535, 2009.

[30]R. de Levie, "The Henderson-Hasselbalch Equation: Its History and Limitations", Journal of Chemical Education, vol. 80, no. 2, p. 146, 2003.

[31] F. Aman-Pommier, G. Degobert and C. Jallut, "Solubility of diazepam in water + tert-butyl alcohol solvent mixtures: Part 1. Experimental data and thermodynamic analysis", Fluid Phase Equilibria, vol. 408, pp. 284-298, 2016.

[32]M. O'Neil, The Merck index. Whitehouse Station, N.J.: Merck, 2006, p. 509.

[33]A. Schneider, C. Pasel, M. Luckas, K. Schmidt and J. Herbell, "Determination of Hydrogen Single Ion Activity Coefficients in Aqueous HCl Solutions at 25°C", Journal of Solution Chemistry, vol. 33, no. 3, pp. 257-273, 2004.

[34]R. Treybal, Mass-transfer operations. New York [u.a.]: McGraw-Hill, 2004.

[35]R. Sheldon, "ChemInform Abstract: The E Factor: Fifteen Years on", ChemInform, vol. 39, no. 14, 2008.

[36]United States Environmental Protection Agency, "Introduction to Hazardous Waste Identification (40 CFR Parts 261)", 2005.

[37]D. Woods, Rules of thumb in engineering practice. Weinheim: Wiley VCH, 2008.

[38]J. Happel and D. Jordan, Chemical process economics. New York: M. Dekker, 1975.

[39]S. Schaber, D. Gerogiorgis, R. Ramachandran, J. Evans, P. Barton and B. Trout, "Economic Analysis of Integrated Continuous and Batch Pharmaceutical Manufacturing: A Case Study", Industrial & Engineering Chemistry Research, vol. 50, no. 17, pp. 10083-10092, 2011.

[40]Food and Drug Administration, "Q3C - Tables and List Guidance for Industry", 2017.

7 Appendix A - Atropine synthesis reaction kinetics

7.1 Simple mechanism

For the first step, by omitting the concentration of H_2O (it is high and not drastically shifted by the reactions):

$$K'_{eq} = \frac{C^*_{10}}{C_{10}C^*_{OH}} \quad (52)$$

For the second and third steps, the rate of reaction is:

$$-r_{10} = k'_{101}C^*_{10}C_{H_2CO} \quad (53)$$

By solving eq. (7) in terms of [10^-] and substituting in eq. (8):

$$-r_{10} = k''_{101}C^*_{10}C_{H_2CO}C^*_{OH} \quad (54)$$

Where C^*_{OH} is the concentration of the hydroxide ion, which is intermediate, and according to the state approximation is considered constant:

$$-r_{10} = k_{101}C^*_{10}C_{H_2CO} \quad (55)$$

7.2 Catalytic mechanism

For the first step:

$$K'_{eq} = \frac{C^*_{10}C_{12}}{C_{10}C^*_{12}} \quad (56)$$

Where C^*_{10}, C^*_{12} are the concentrations of the intermediate ions.

For the second and third steps, by substituting eq. (11) into eq. (8), the rate of reaction is:

$$-r_{10} = k'_{101}\frac{C_{10}C_{H_2CO}C^*_{12}}{C_{12}} \quad (57)$$

According to the steady-state approximation, C^*_{12} is the concentration of an intermediate and thus considered constant:

$$-r_{10} = k''_{101}\frac{C_{10}C_{H_2CO}}{C_{12}} \quad (58)$$

Using the definition of yield:

$$C_{12} = Y_{\frac{12}{10}}(C_{10,0} - C_{10}) \quad (59)$$

For constant yield and by substituting eq. (14) into eq. (13):

$$-r_{10} = k_{101}\frac{C_{10}C_{H_2CO}}{C_{10,0}-C_{10}} \quad (60)$$